

Towards Improved Multi-Hazard Risk
Assessment: Challenges and Applications for
Java, Indonesia

Name: Renée van der Knaap (2617069)

21/07/2024

Thesis Supervisor: Eric Koomen

Preface

Before you lies my master thesis “Towards Improved Multi-Hazard Risk Assessment: Challenges and Applications for Java, Indonesia”, written for completion of the MSc Spatial, Transport and Environmental Economics. It has been a long journey, but I am very happy and proud to have finished this thesis. I learned a lot from this thesis and its process, and I hope to make use of these valuable lessons in the future.

There are a few people who helped me tremendously throughout the process of writing my thesis, and I would like to thank them in this preface. First and foremost, I would like to thank my thesis supervisor Eric Koomen. I greatly appreciate your enduring supervision and support throughout this process, which lasted longer than usual. Therefore, I would also like to thank Eric for his patience and understanding. I could not have asked for a better thesis supervisor in my situation. Thank you, Eric! Additionally, I would like to thank academic advisor Nick Oskam, who supported me throughout the process. I greatly appreciate your help, by thinking along with me in planning the work on my thesis and in staying motivated to finish this thesis. Lastly, I want to thank my father, Wim van der Knaap, who helped me finalizing my thesis and giving me some extra motivation in the last part of my thesis.

Abstract

The topic of natural hazards is becoming increasingly relevant, as climate change is affecting their intensity and frequency. There are many countries exposed to multiple hazards, leading to great risk of experiencing catastrophic damages. Multi-hazard risk assessments can help identifying the possible damages and therefore help mitigate future multi-hazard risk. Currently, methodologies for multi-hazard risk assessments are in the development stage and there is thus need for improvement. It appears that hazard and impact interaction are crucial aspects of multi-hazard risk assessment, but multi-hazard frameworks lack standardization of these conditions. There is need for improvement of these frameworks, by extending them with methodologies for hazard and impact interaction calculations. This way, appliance of multi-hazard risk frameworks can lead to more accurate risk assessments and therefore contribute to risk management.

Table of Contents

1. <i>Introduction</i>	5
2. <i>Literature review</i>	7
2.1 Existing methods	7
2.1.1 Hazard interactions	7
2.1.2 Examples of multi-hazard risk assessments	8
2.1.3 Multi-hazard frameworks	9
2.2 Conclusion and research gaps.....	11
2.3 Contribution to closing the research gaps.....	13
3. <i>Setting up the multi-hazard risk assessment for the case study</i>	14
3.1 Description of the case study area	14
3.2 Identifying multi-hazard scenarios and their hazard interactions	15
3.3 Risk calculation	15
3.3.1 Exposure analysis	16
3.4 Independent hazards scenario: hazard, vulnerability and expected annual loss	18
3.5 Cascading hazards scenario: hazard, vulnerability and expected annual loss.....	21
3.6 Data sources.....	23
3.6.1 Data collection and pre-processing.....	23
3.6.2 Data quality	24
4. <i>Results of the multi-hazard risk assessment</i>	26
4.1 Hazard susceptibility analysis.....	26
4.2 Scenario of independent hazards.....	27
4.3 Scenario of cascading hazards	29
4.4 Comparison between independency scenario and cascading scenario	30
5. <i>Conclusion and discussion</i>	31
5.1 Conclusion.....	31
5.2 Discussion	32
<i>References</i>	35
<i>Appendix</i>	40
A. Summarizing table of spatial data sources used for this research	40
B. Maps of the original hazard datasets used in the two multi-hazard scenarios	41
C. Original land-use dataset.....	43

1. Introduction

Natural hazards are an integral part of life on earth, as they heavily affect people and their environment (Leroy, 2006). Due to climate change, the understanding and mitigation of natural hazards is of great importance, as climate change increases the intensity and frequency of natural disaster events (European Environment Agency, 2017; Negulescu, et al., 2023). In addition, an increase in economic exposure, driven by population and economic growth, is expected to increase the risk of losses due to natural hazards, particularly in disaster-prone regions (Botzen, Deschenes, & Sanders, 2019). This growth leads to more built-up areas, putting more lives and economic assets at risk.

Although many natural hazard risk assessments have been performed in the past, less is known about the risk of multiple hazards in a given area (Sadegh, et al., 2018; Nugroho, Triana, Fitrah, & Hamid, 2022). Nevertheless, many countries experience multiple types of natural hazards and are prone to economic losses due to multi-hazard risk (World Environment Situation Room, 2023; Dilley, et al., 2005). According to Dilley et al. (2005), 3.4 billion people are exposed to at least one hazard, 790 million people are exposed to at least two hazards and 105 million people are exposed to at least three or more hazards. These numbers have likely increased over the past two decades due to population growth and urbanization (De Angeli, et al., 2022).

Within the concept of multi-hazard risk, several subdivisions exist, such as compound risk (simultaneous or successive hazards with a possible shared origin) and cascading risk (one hazard triggering others) (Cutter, 2018; Pescaroli & Alexander, 2018; Ahamed, Sarmah, Dabral, Chatterjee, & Shaw, 2023; Gissing, Timms, Browning, Crompton, & McAneney, 2022). Ahamed et al. (2023) addressed the fact that not every researcher uses the exact same definition of these concepts. Moreover, different types of hazard interactions are considered, such as parallel relationships (where changes in trigger factors can induce multiple hazards) and mutex relationships (where hazards have opposing trigger factors and cannot occur together) (Liu, Siu, & Mitchell, 2016; De Angeli, et al., 2022).

The methodologies used in multi-hazard risk assessments vary widely as well (De Angeli, et al., 2022). Due to the early stage of development of analysing multi-hazard risk, methodologies are often simplified while multi-hazard risk is actually a very complex subject. When obtaining a multi-hazard risk assessment, some studies do not take the hazard interactions and/or impact interactions into account. For example, Aksha et al. (2020) analysed three hazards individually and then overlaid the individual maps to create the multi-hazard map. Additionally, they did not account for impact interactions.

It is thus important to have a clear overview of terminology, and consider aspects like hazard interaction and impact interaction. This way, researchers can make use of a fitting methodology to obtain accurate multi-hazard risk assessments. Using correct methods, the risk analysis can be performed as accurate as possible and policies can be implemented in such a way that they are most effective. Therefore, the goal of this research is to find a proper methodology to perform a multi-hazard risk analysis of a case study and to contribute to improvement of multi-hazard risk assessment. For this to be achieved, the following main research question will be examined:

What are important aspects to improve in multi-hazard risk assessment methodologies?

The main research question is supported by three sub-questions:

1. *Which methods are used in previously performed research?*
2. *What are the current challenges in multi-hazard risk assessment?*
3. *What can we learn from the appliance of these methods to a new case study area, by comparing two scenarios of different hazard interactions?*

To answer these questions, a literature review will be performed first to gain more knowledge about multi-hazard risk assessment. The review will focus on the development of methodologies within this concept, and how previously used approaches can be improved and combined to contribute to the progress of multi-hazard risk assessment. The composed methodology will be applied to a case study in Indonesia, specifically the island of Java, where approximately 40% of the inhabitants of Indonesia are at risk of multiple hazards. Java is a densely populated island in Indonesia, and is one of the islands in Indonesia which is the most prone to multiple hazards (World bank, 2021). In addition, the economic losses due to natural hazards in Indonesia are tremendous. According to Berkeley Economic Review (2019), Indonesia has lost around 3.5 trillion US dollars between 1989 and 2019, to the consequences of natural hazards.

The structure of this thesis is as follows: Chapter 2 provides a comprehensive literature review discussing existing methods and identifying research gaps. Chapter 3 outlines the application of the methodology to the multi-hazard risk assessment. Chapter 4 presents the results of this assessment. Finally, the conclusion and discussion can be found in Chapter 5.

2. Literature review

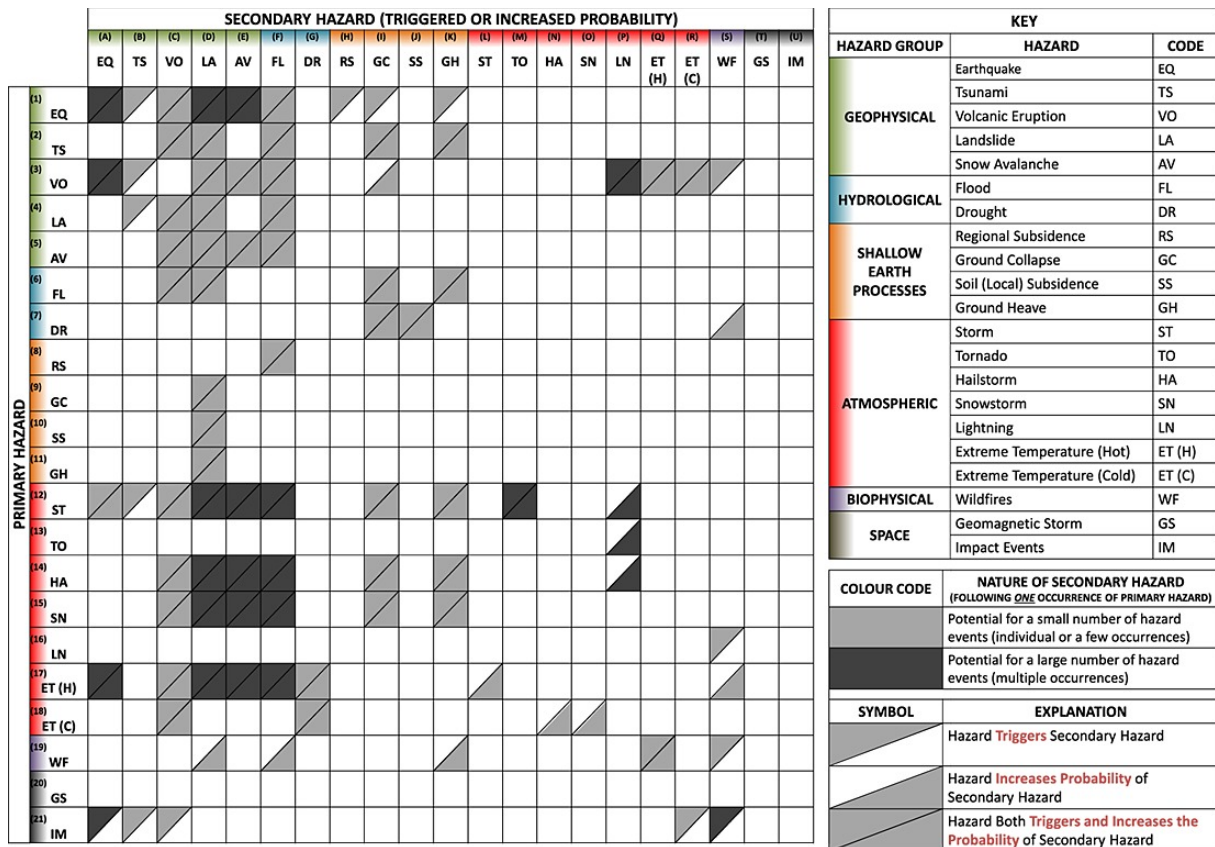
Several authors have reviewed available methods for multi-hazard risk assessment (Gallina, et al., 2016; Ciurean, Gill, Reeves, O'Grady, & Aldridge, 2018; Tilloy, Malamud, Winter, & Joly-Laugel, 2019; Wang, He, & Weng, 2020; Hochrainer-Stigler, et al., 2023). As addressed in the introduction, the terminology within the concept of multi-hazard (risk) varies amongst researchers. From the reviewed articles it appears that, in addition to the terminology not being universal, the methodologies available for multi-hazard risk assessment are still in the development stage. In the following sections, several existing methodologies for multi-hazard risk assessment are discussed (Section 2.1), to identify research gaps (Section 2.2) and ultimately discuss the contribution of this research to the research gaps found in the literature (Section 2.3).

2.1 Existing methods

In this section, existing methods are reviewed. First, background information on finding the relationships between natural hazards is discussed (Paragraph 2.1.1). This is followed by examples of previously performed multi-hazard risk assessments (Paragraph 2.1.2). Finally, studies that constructed frameworks for application in a multi-hazard risk assessments are discussed (Paragraph 2.1.3).

2.1.1 Hazard interactions

The interrelationships between natural hazards have been intensively studied by Gill & Malamud (2014). Understanding these interactions within a multi-hazard scenario is an essential foundation for the initial steps of risk assessment. Natural hazards can arise from specific geophysical environments, influenced by environmental factors in the atmosphere (Liu, Siu, & Mitchell, 2016; Gill & Malamud, 2014). The similarities in geophysical environments can lead to several hazard interactions: one hazard can increase the probability of a second hazard occurring, or one hazard can trigger multiple hazards. Gill & Malamud (2014) provided a characterization and visualization of hazard interactions for 21 different hazards (Figure 1). In their matrix, the shaded upper left triangle in each "cell" represents the case in which a primary hazard could trigger a secondary hazard, and the shaded bottom-right triangle represents the case in which a primary hazard could increase the probability of a secondary hazard being triggered. Light grey triangles indicate that the primary hazard can trigger or increase the probability of a few or single occurrences of the secondary hazard, while dark grey triangles indicate that the primary hazard can trigger or increase the probability of multiple occurrences of the secondary hazard (Gill & Malamud, 2014).



Footnotes

- [1A,D,E; 3A,P; 12D-F,M,P; 13P; 14D-F,P; 15D-F; 17A,D-F; 21A] The secondary hazards in these cases are all accepted to most likely occur as large numbers of events, and are thus analysed in this way.
- [1C] There is disagreement in the literature about the nature of this relationship .
- [2,6,12,14,15C] Water input triggers or increases the probability of a phreatic/phreatomagmatic eruption.
- [3I] Volcanism increases the acidity of rain, promoting dissolution of carbonate material.
- [12A] Low pressure systems have been shown to trigger or increase the probability of slow earthquakes on faults that are already close to failure (Liu *et al.*, 2009).
- [17A,C-F] Secondary hazards triggered or have an increased probability over a range of time-scales, through snow and glacial melting.
- [18C] Long term reductions in temperature can increase glaciation and thus decrease sea-levels. This reduction in sea-levels can reduce confining pressures, promoting volcanic eruptions.

Figure 1: Identification of hazard interactions, for 21 hazards. The vertical axis depicts the primary hazard and the horizontal axis depicts the secondary hazard (Gill & Malamud, 2014).

2.1.2 Examples of multi-hazard risk assessments

The studies for the review are selected based on the following criteria: published in or after 2020; performing an assessment of multiple hazards; applying the assessment on a case study area; variety between the studies in addressing the interrelations. In this paragraph, three examples of multi-hazard risk assessments are shortly discussed. In Paragraph 2.1.3, three examples of multi-hazard frameworks are shortly discussed.

The first example is from Zhang, Hao & Zhang (2023). They performed an agricultural risk assessment of compound dry and hot events (CDHEs) in China. They used historical data to simulate the future agricultural risk of CDHEs. The risk was calculated using hazard, exposure and vulnerability. The hazard was defined as the frequency of CDHEs (considered as a single hazard), the exposure as the proportion of cropland, and the vulnerability as the irrigated area fraction and GDP. By combining these factors, the expected future agricultural risk of CDHEs was obtained.

The second example is a study from Aksha, Resler, Juran & Carstensen (2020), who investigated the multi-hazard risk in the city of Dharan, Nepal. They performed separate hazard assessments for

landslides, floods and the earthquake, followed by creating an integrated hazard map after weighting and ranking each individual hazard type. Subsequently, a vulnerability map was created and multiplied with the integrated hazard map to obtain an overall risk assessment.

Lastly, Randell, Jiang, Liang, Murtugudde & Sapkota (2021) performed a study about food insecurity and compound environmental shocks in Nepal, focusing on the compound events of an earthquake and monsoon season (leading to landslides/flooding) in 2015. They created a map of Nepal indicating the intensity of the earthquake and the level of rainfall based on deviations from rainfall during a baseline period. Subsequently, a set of binary logistic regressions were estimated to find the likelihood of moderate or severe food insecurity, with the earthquake intensity and rainfall as the main predictors.

In the methods discussed above, the authors did not consider interrelationships between hazards. In multi-hazard risk assessment, it is crucial to consider both the interrelationships between hazards and the impact from multiple hazards (Hochrainer-Stigler, et al., 2023). For example, Zhang et al. (2023) did not account for changes in risk due to hazard and/or risk interaction, as there is a possibility of combined impacts on, in this case, agricultural land caused by droughts and hot extremes. Aksha et al. (2020) acknowledged the importance of hazard interactions for multi-hazard risk assessment but did not incorporate this due to a lack of historical data. Randell et al. (2021) considered interactions between hazards and both individual and additive impacts more comprehensively.

2.1.3 Multi-hazard frameworks

More comprehensive frameworks composed for multi-hazard risk assessment are discussed next, with examples from Liu, Siu & Mitchell (2016), De Angeli et al. (2022) and Hochrainer-Stigler et al. (2023).

Liu et al. (2016) developed a framework to classify hazard interactions based on the so-called hazard-forming environment. They defined two types of geophysical environmental factors influencing natural hazards: stable factors (preconditions of the hazard which never or hardly change, such as tectonic plates) and trigger factors (constantly changing, such as temperature or wind speed). The authors provided a list of natural hazards and their stable and trigger factors, and illustrated their developed framework in a flowchart (Figure 2), as well as the relationships between hazards (Figure 3).

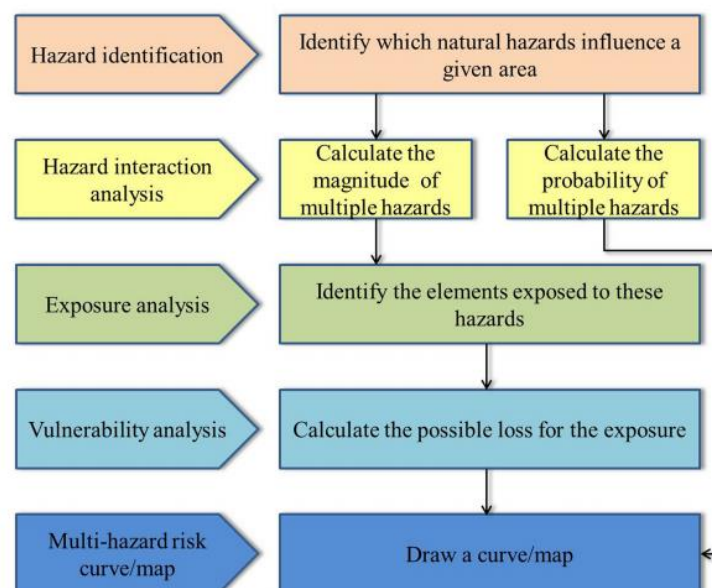


Figure 2: Framework of multi-hazard risk assessment (Liu, Siu & Mitchell, 2016).

Liu et al. (2016) applied their framework to a region in China, where the region is divided into different zones based on the number and types of hazards occurring in that zone. Also, the susceptibility of each area to each hazard is calculated based on the stable factors. Subsequently, the hazard interactions in the zones are analysed, based on trigger factors. This is followed by calculations of the exceedance probabilities of the corresponding trigger factors, based on the mathematical statistics approach using data of the trigger factors during each historical hazard occurrence. This analysis is followed and finalized by defining exposure and vulnerability indicators, to obtain the multi-hazard risk: A map of the loss distribution with different exceedance probabilities.

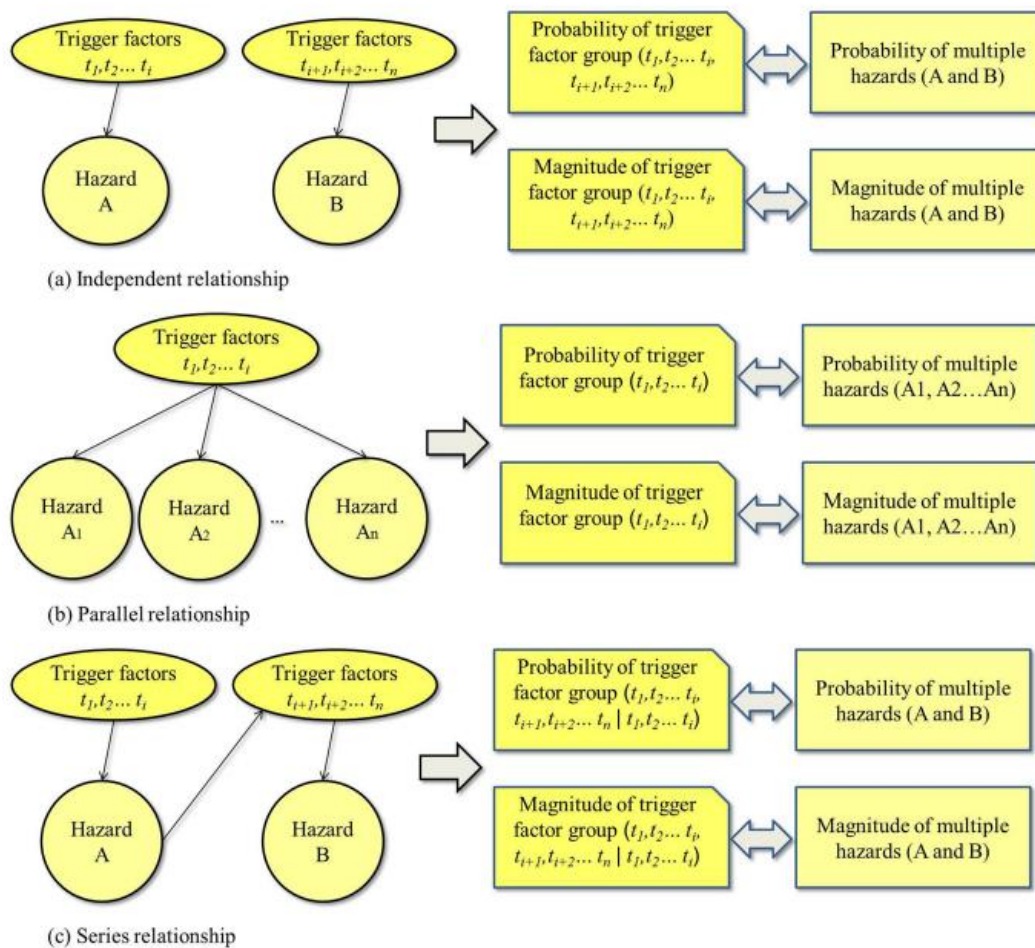


Figure 3: Hazard interaction analysis for hazards with different relationships (Liu, Siu & Mitchell, 2016).

A critical literature review of multi-hazard risk approaches was performed by De Angeli et al. (2022), to develop a framework for multi-hazard spatial-temporal impact analysis, consisting of five steps (Figure 4). The authors also found that there is a fairly great variety of multi-hazard definitions between different scientists, including variety in classification of hazard interaction types. By combining these definitions and finding similarities between authors, De Angeli et al. (2022) identify six different hazard interaction types, to use for the first step of the framework.

To visualize the multi-hazard impact framework, it was applied to a case study in the Po river valley in Italy, based on a project performed by RASOR (RASOR Project, 2013). This valley experienced an earthquake in 2012, weakening the local levee system and other flood defences were damaged. As a consequence, the Po valley was increasingly susceptible to flooding. The hypothetical scenario discussed by De Angeli et al. (2022) involved heavy rains occurring nine days after the earthquake, causing the river to flood.

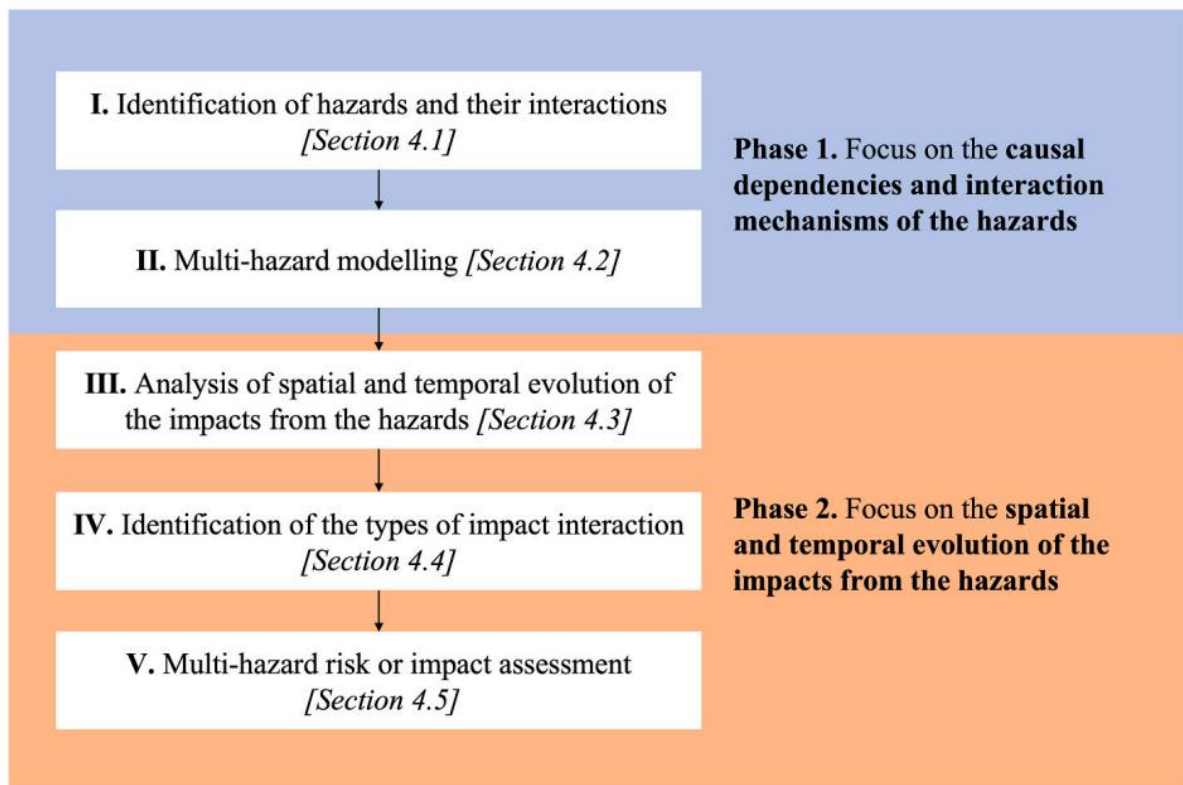


Figure 4: The five-step multi-hazard impact framework developed by De Angeli et al. (2022).

Hochrainer-Stigler et al. (2023) proposed a more extended framework that addresses single- and systemic risk, multi-risk analysis, and risk management. Their framework consists of six steps:

1. Finding a system definition (i.e. determining the hazards and characterizing “governance landscape” for management)
2. Characterization of direct risk
3. Characterization of indirect risk (i.e. indirect risk due to interdependencies in the systems)
4. Evaluation of direct and indirect risk
5. Defining risk management options
6. Accounting for future system state

The framework of Hochrainer-Stigler et al. (2023) certainly has some similarities with the frameworks of Liu et al. (2016) and De Angeli et al. (2022), such as accounting for hazard interactions and impact interaction. However, it also includes systemic risk and takes into account risk management, which makes the framework rather complex. This complexity is also acknowledged by the authors.

2.2 Conclusion and research gaps

There are two main conclusions which can be drawn from the literature review. First, there is no standard glossary for hazard interactions, resulting in various terms for similar concepts. However, this will not be further discussed in this research. Second and relevant for this study, authors perform multi-hazard risk assessments without taking into account the hazard and impact interactions. Related to this second conclusion, the spatial analysis of multiple hazards lacks accuracy. Consequently, the review of the literature reveals several research gaps and areas for improvement. Table 1 provides an overview of the discussed literature, indicating whether or not the authors considered interrelationships.

Table 1: Summarizing table of the reviewed literature concerning multi-hazard risk.

	Number and types of included hazards	Addresses interrelationships in probability of occurrence	Addresses interrelationships in impact (e.g. damage)
(Zhang, Hao, & Zhang, 2023)	2; Compound drought and heat events	Yes (takes the simultaneous occurrence of two events as one)	No
(Aksha, Resler, Juran, & Carstensen Jr, 2020)	3; Flood, landslide and earthquake	No	No
(Randell, Jiang, Liang, Murtugudde, & Sapkota, 2021)	2; Earthquake and monsoon rainfall leading to food insecurity	No	Yes
(Liu, Siu, & Mitchell, 2016)	Up to 6; Landslide, strong wind and floods (4 types)	Yes	Yes
(De Angeli, et al., 2022)	2; Earthquake and flooding	Yes	Yes
(Hochrainer-Stigler, et al., 2023)	No empirical example	Framework: Yes	Framework: Yes

The first three articles presented somewhat simplified methodologies, as they performed risk assessments for each hazard individually without considering interrelationships between hazards and/or impacts. Conversely, the reviewed frameworks for multi-hazard risk assessment include steps that identify hazard and impact interactions. However, there are still some research gaps within multi-hazard risk assessment, also acknowledged by the authors themselves. I define two research gaps based on the literature review.

First, it is important to improve the methodologies for multi-hazard risk assessments considering hazard- and impact interactions. De Angeli et al. (2022) highlighted limitations in steps 2 (hazard modelling) and 5 (impact assessment) of their framework, noting the difficulty in defining standardized procedures for these steps. It is challenging to define a standardized procedure for step 2, because of the variety and heterogeneity of different hazards and their interactions. Similarly, De Angeli et al. (2022) stated that they did not find a standardized way to calculate multi-hazards impacts in the literature, due to the variety and heterogeneity of different interaction types.

Second, in the application of the framework by Liu et al. (2016), the authors made use of the administrative borders of counties to determine the hazards susceptibility in a specific county. However, this ignores the spatial distribution of hazards that is often more refined than the boundaries of the administrative units suggest. For example, Röthlisberger, Zischg & Keiler (2017) stated that the aggregation based on grid cells supports the comparability of different regions better than aggregation based on municipalities, in their study on flood exposure. This spatial mismatch relates to the well-known Modifiable Areal Unit Problem (MAUP) introduced by Openshaw (1984).

2.3 Contribution to closing the research gaps

This research aims to address the two gaps mentioned in Section 2.2 by applying a combination of the frameworks constructed by De Angeli et al. (2022) and Liu et al. (2016) to a new case study area. These frameworks both include interrelationships between hazards as well as between impacts. As mentioned in Paragraph 2.1.3, the framework of Hochrainer-Stigler et al. (2023) is rather complex. Therefore, the framework will not be used in this research but it is important to mention that it accounts for and gives good insights in many aspects within the concept of multi-hazard risk assessment and management.

An important gap to close in multi-hazard risk assessments is determining hazard interactions, and taking those interactions into account in terms of the probability of a multi-hazard scenario. I will contribute to closing this gap by applying a multi-hazard risk assessment to two different scenarios of hazard interaction, as different hazard interactions require different assessment methodologies. Two important hazard interactions which are distinct in assessment methodologies are independent relations and triggering (cascading) relations (De Angeli, et al., 2022; Liu, Siu, & Mitchell, 2016). Therefore, these relations will be examined in the multi-hazard risk assessment. Additionally, I will address the importance of taking possible impact interactions into consideration. In terms of increasing accuracy in the risk assessment, I will calculate the risk per pixel/grid cell rather than per district, region or country.

Overall, this research will provide insights on the applicability of existing frameworks to other case study areas and help improve the construction of new or adjusted multi-hazard risk assessment frameworks.

3. Setting up the multi-hazard risk assessment for the case study

This chapter outlines the methodology applied in the multi-hazard risk assessment for the case study area. The six key steps in the multi-hazard risk assessment include:

1. Hazard susceptibility analysis: Identifying which natural hazards influence the province of Java
2. Identification of hazards and their interactions to define two different multi-hazard scenarios for the risk assessment
3. Exposure analysis
4. Identification of the scenario (or hazard) probabilities and of the spatial overlap between the hazards
5. Vulnerability analysis
6. Multi-hazard risk assessment: Determination of the Expected Annual Loss

First, a description of the case study area is given to gain background knowledge about the study area and understand the choice of study area for this research, in Section 3.1. This is also an introduction to the first step in the multi-hazard risk assessment, namely finding the susceptibility to natural hazards. The second step of identifying hazards and their interactions is discussed in Section 3.2. In Section 3.3, the risk calculation is introduced together with the elaboration of step 3. Subsequently, step four till six are performed for the two different hazard interaction scenarios (independent and cascading hazard relations), and discussed in Sections 3.4 and 3.5. Chapter 3 finishes off with Section 3.6, which elaborates on the spatial data sources used for this multi-hazard risk assessment.

3.1 Description of the case study area

The case study focuses on the island of Java, Indonesia (Figure 5). Java, with a population exceeding 150 million in 2020, constitutes approximately 56% of Indonesia's population (Statista, 2022) and contributes around 57% to the national GDP in the third quarter of 2023 (BPS-Statistics Indonesia, 2023). In regard to natural hazards, between 1980 and 2020, Indonesia primarily experienced the following natural hazards: Earthquake; Flood (River and Coastal); Landslide; Volcanic activity; Drought; Storm; Mass movement (dry); Wildfire (World bank, 2021). According to the Centre for Hazards and Risk Research at Columbia University (2005), Java and Sumatra experience the highest GDP impact and mortality rates from multi-hazard risks.



Figure 5: Location of the case study area Java, Indonesia (background map is retrieved from OpenStreetMap tiles (2024)).

A map illustrating the topographic distribution of seven natural hazards was generated (discussed in Chapter 4), focusing on the mainland of Java, excluding smaller islands (less than 1,000 square kilometres). The seven hazards which are used for the map are: Coastal flood; River flood; Landslides triggered by precipitation (Landslides Pr.); Landslides triggered by earthquakes (Landslides Eq.); Earthquake; Wildfire; Volcanic hazard (excluding ash fall). Due to the time and resources available for this research, the multi-hazard risk assessment will not be performed for all of the above hazards. In the next section, I discuss to which hazards the risk assessment will be applied to and how.

3.2 Identifying multi-hazard scenarios and their hazard interactions

To perform a feasible multi-hazard risk assessment, the analysis is not continued for all seven hazards mentioned in Section 3.1. Based on data availability (feasibility), occurrence of the hazards on Java (Figure 9 and Table 9) and possible hazard interaction, three hazards have been chosen to perform a risk assessment for two multi-hazard scenarios.

Based on the hazard interactions mentioned in Chapter 2 (Gill & Malamud, 2014) and the results of the susceptibility analysis in Section 4.1 (Figure 9 and Table 9), the multi-hazard risk assessment will proceed with the following natural hazards: *Landslide (triggered by earthquake and precipitation combined); Earthquake; and Wildfire*. The most frequent combination of hazards is: Landslide Eq., Landslide Pr., Earthquake, Wildfire and Volcanic hazard, which overlap spatially for highest percentage of land area (46%; Table 9). Volcanic hazard is not taken into account in this risk assessment, due to data availability and data quality.

There are several interactions between the three chosen hazards. Following Gill & Malamud (2014), earthquakes can both trigger and increase the probability of landslides, while landslides do not trigger or increase the probability of earthquakes. Earthquakes do not trigger or increase the probability of wildfires, and wildfires do not trigger or increase the probability of wildfires. Wildfires can increase the probability of a landslide, but landslides do not trigger or increase the probability of a wildfire (Gill & Malamud, 2014). There exists no trigger between earthquakes and wildfires, but the hazards can occur together (i.e. they do not exclude each other).

The two different hazard interaction scenarios are as follows: One scenario, where an earthquake and a wildfire occur together; and another scenario, where an earthquake and landslides occur together. These two scenarios differ in hazard interaction as well as in impact interaction. As discussed in the introduction and literature review, there exists a wide range of used terminology for different hazard interactions. This research will follow the paper of De Angeli et al. (2022), which defines six hazard interactions with causal dependencies, and the paper of Tilloy et al. (2019), which also defines an independent relationship between hazards. As discussed above, no trigger exists between earthquakes and wildfires (Gill & Malamud, 2014). The hazard interaction in the first scenario is thus “Independence” (Tilloy, Malamud, Winter, & Joly-Laugel, 2019). Between earthquakes and landslides, there does exist a trigger. The hazard interaction in the second scenario is “Cascading” (De Angeli, et al., 2022). The identification of the impact interaction is discussed in Paragraph 3.5.2.

3.3 Risk calculation

To determine the damage in each scenario, the expected annual loss was calculated. This calculation was done based on an equation from FEMA (2024):

$$EAL = Exposure * Annualized Frequency * Historic Loss Ratio \quad (1)$$

where EAL is the expected annual loss, exposure is the value of assets (or people) which could be damaged, the annualized frequency is the expected frequency of the occurrence of the natural hazard per year and the historic loss ratio is the estimated percentage of the exposure expected to be lost due to the natural hazard (FEMA, 2024). It is crucial to express the damages in the multi-hazard risk assessment in a unit which can be determined for all individual natural hazard types, to ultimately find the accumulated final total of damages. All values of expected annual loss should have a common unit of measurement (Zuzak, et al., 2023). In this study, the unit of the exposure values will be US Dollars determined in areas of one hectare, leading to a unit of US Dollars per hectare for the expected annual loss.

For the remainder of this report, the annualized frequency will be referred to as “(natural) hazard” and the historic loss ratio will be referred to as “vulnerability”. Natural hazard can be defined as “Natural process or phenomenon that may cause loss of life, injury or other health impacts, property damage, loss of livelihoods and services, social and economic disruption, or environmental damage”, according to UNISDR (2009). Vulnerability can be defined as “The characteristics and circumstances of a community, system or asset that make it susceptible to the damaging effects of a hazard”, according to UNISDR (2009). These characteristics also determine the estimated percentage of the asset to be lost due to a natural hazard, as the historic loss ratio was described.

3.3.1 Exposure analysis

To calculate the expected annual loss, first the exposure on the island of Java needs to be determined. Like done in previous risk assessment studies, for example by (Baky, Islam, & Paul, 2020), different land-use classes will be used to identify the elements at risk. In this study, I apply a dataset derived from the Copernicus institute that represents land use in 2019 (more details in Appendix A). The elements at risk consist of Urban Area, Cropland and Forest (Figure 6). These categories represent the primary land uses on Java. As can be seen in Figure 6, remaining land uses are categorized by “other”, which is neglected in the calculations of the expected annual loss as it is hard to determine a monetary value (exposure) and damage rate (vulnerability) for this category.

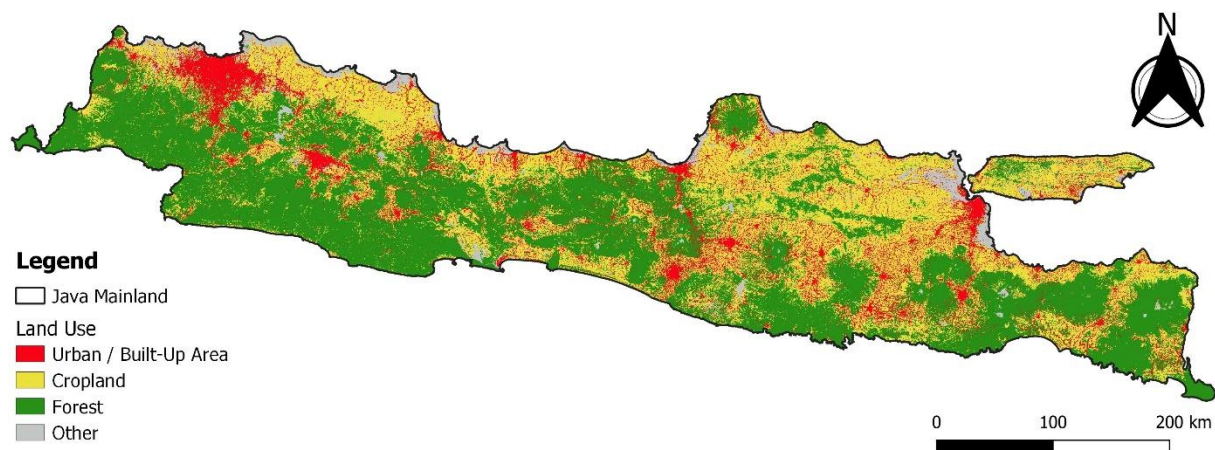


Figure 6: Land-use map of Java, using four land-use categories.

For each of the three land-use classes, a monetary value is obtained. For cropland and forest, this was done based on the study of Kiely et al. (2021), which was conducted in Indonesia. Kiely et al. (2021) also used land cover data to determine the elements at risk, and estimate the value of land based on the Net Present Value (NPV). For the land-use class forest, they used a value of \$4079 per hectare

based on provisioning, regulating and cultural services of forest. For cropland, a value of \$827 per hectare was used. The values used in this study are summarized in Table 2.

Table 2: Net Present Value (NPV) of forest and cropland on Java.

	NPV per hectare (US Dollars)
Forest	4079
Cropland	827

To determine the monetary value of urban area, the annual Gross Regional Domestic Product (GDP) by province in 2023 was used (BPS-Statistics Indonesia, 2024). According to Ward et al. (2020), GDP is one of the most commonly used data to represent exposure in natural hazard risk assessments. The sector of Agriculture, Forestry and Fishing is subtracted from the total GDP to prevent double counting of the agriculture (cropland) and forest values. In Table 3, the calculations for the GDP per province on Java can be seen. For the final calculations performed in GIS, the regional GDP needs to be converted to GDP per hectare. This is done by dividing the GDP of a province by the amount of urban area present within the province (Table 4).

Table 3: Calculations of annual GDP (2023) of provinces in Java, used as monetary value of urban area, retrieved from BPS-Statistics Indonesia (2024). Values in Rupiah are converted to US Dollar based on the average exchange rate of 2023¹.

	Total annual GDP Region (billion rupiah)	Agriculture, forestry, fishing. (billion rupiah)	GDP minus agriculture, forestry, fishing (billion rupiah)	GDP minus agriculture, forestry, fishing (billion US dollars ²)
Dki Jakarta	2,050,466.0	1,442.0	2,049,023.9	134.5
Banten	507,427.2	26,524.0	480,903.2	31.6
Jawa Tengah	1,102,563.2	131,397.5	971,165.7	63.7
Jawa Timur	1,844,808.7	177,632.3	1,667,176.4	109.4
Jawa Barat	1,669,416.9	113,308.5	1,556,108.3	102.1
Di Yogyakarta	118,626.8	9,171.1	109,455.7	7.2

Table 4: Amount of urban area present in the six provinces on Java, and the corresponding value of GDP.

	Total urban area (hectares ³)	GDP (US dollar per hectare)
Dki Jakarta	60,241.4	2,223,377.2
Banten	108,590.7	289,495.9
Jawa Tengah	450,209.2	141,093.3
Jawa Timur	600,416.6	181,526.1
Jawa Barat	437,750.6	232,572.5
Di Yogyakarta	54,551.0	131,289.4

In conclusion, the monetary value of forest and cropland is based on the Net Present Value (Table 2) and the monetary value of urban area is based on the regional GDP (Table 4). It should be appointed that for the land uses forest and cropland one value was used for the whole island. This is in contrast

¹ <https://www.exchange-rates.org/exchange-rate-history/idr-usd-2023>

² One rupiah is equal to 0.00006564 US dollar

³ The total amount of pixels of urban area is multiplied by the size of the pixel, 1.22611329 hectare

to the value of urban area, which is dependent on the location on the island, as a distinction is made between provinces. This is done based on the assumption that forest and cropland do not significantly differ between regions within the island. However, the urban value (GDP) can differ significantly between regions. For example, there can be a difference in the economy of a city and its development level, but also in size. Dki Jakarta has a relatively small amount of urban area but the GDP is very high compared to Jawa Timur. In addition, Dki Jakarta and Di Yogyakarta have roughly the same amount of urban area but tremendous differences in GDP (Table 4). If there was just one monetary value used for urban area, some locations would get an overestimation and others an underestimation in expected losses. Therefore, the regional GDP has been used to define the monetary value of urban area, such that the value of urban land preserves its spatial pattern.

3.4 Independent hazards scenario: hazard, vulnerability and expected annual loss

In the first scenario, the risk of an independent hazard interaction of an earthquake and wildfire on the Island of Java is assessed. Having previously determined exposure on Java, this section focuses on determining hazard and vulnerability to complete Equation 1. Additionally, the spatial overlap of hazards is determined, following De Angeli et al. (2022).

Figure 7 illustrates the spatial overlap of earthquake and wildfire hazards, highlighting the most hazardous areas. This can be helpful in the understanding of the spatial patterns of the expected annual loss in scenario A, discussed in the next chapter. To calculate the EAL, one of the required components is the hazard data. For the earthquake hazard, Peak Ground Acceleration (PGA) data of an earthquake with a return period of 475 years is used, giving a 0.21% annual probability. For the wildfire hazard, data of historic wildfires on Java in the past 20 years has been used, which gives the annual frequency of fires per square kilometre. As these two hazards are independent from each other, the hazard probabilities of the earthquake and wildfires can be simply added together.

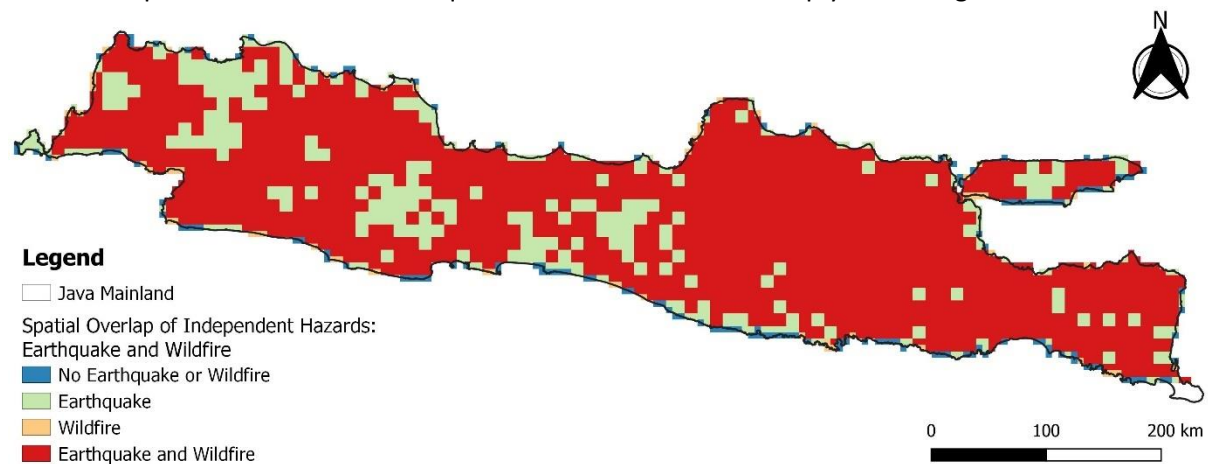


Figure 7: Spatial overlap of an earthquake and wildfires on Java, in the independent hazards scenario.

In terms of the vulnerability of the elements at risk to earthquakes and wildfires, there are differences both between the hazards and between the land-use classes. In this study, the vulnerability of cropland is assumed to be the same as the vulnerability of urban area, due to lack of data about the vulnerability of cropland to an earthquake. It is assumed that the infrastructure and machinery present on cropland have similar vulnerability to urban area. This assumption extends to wildfires and landslides for consistency.

3.4.1 Earthquake vulnerability

First, the vulnerability of the land-use classes to earthquakes will be discussed. For urban area, a combination of the studies of Naguit et al. (2017) and Fujimi & Aulady (2019) was used to determine the damage rates per intensity of the earthquake. Naguit et al. (2017) provides damage rates for building types in the Philippines, assumed to be similar to Indonesia. There are four building types for which Naguit et al. (2017) created damage curves, which are presented in Table 5, with the intensity of the earthquake accordingly. The average of the rates of the buildings was applied in the final calculation for the EAL. To create more accuracy in the assumption that these rates can be used for Java, a weighted average was applied based on Fujimi & Aulady (2019). They performed research on a part of Java, in which they include percentages of the types of buildings present (Table 5). Combining these two studies leads to the total weighted average shown in Table 6, which are used as the vulnerability rates of urban area and cropland to earthquakes.

Table 5: Building types from two different studies. The percentages in the right column represent the fraction of building types present in the case study area of Fujimi & Aulady (2019).

Naguit et al. (2017)	Fujimi & Aulady (2019)
Confined Masonry	Confined Masonry (53.89%)
Concrete hollow blocks	Reinforced concrete low rise and medium rise (3.59% + 14.97% = 18.56%)
Half-masonry/half-wood	Unreinforced masonry (18.86%)
Wood, light frame	Timber frame (8.68%)

Table 6: Identification of the vulnerability rates of urban area to the earthquake⁴.

	MMI 6	MMI 7	MMI 8
Confined Masonry	10%	23%	38%
Concrete Hollow Blocks	22%	45%	66%
Half-Masonry/Half-Wood	10%	21%	35%
Wood, Light Frame	7%	14%	25%
Total weighted average	11.97%	25.92%	41.50%

To find vulnerability rates of forest, two studies of Allen (1999) and Allen (2020) about tree mortality have been used. In both articles, damages done by previous earthquakes are examined and the tree mortalities are based on the distance from the epicentre of the earthquake. For example, Allen (1999) observed a magnitude of 6.7 (which is approximately equal to an MMI of 8) corresponding to a tree mortality of 24% close to the epicentre, but a tree mortality of 0.6% further away from the epicentre. Assuming the MMI is the highest around the epicentre and declines with distance to the epicentre, the assumption is made that the tree mortality declines with the MMI. The averages are taken from both articles, to get a final total average per MMI to apply as a vulnerability rate of forest (Table 7).

⁴ The values of PGA are converted to the Modified Mercalli Intensity (MMI) scale (Volcano Hazards Program, 1905). In the earthquake data, PGA (g) values are given as intensities. These values are converted based on ranges from Wald, Quitoriano, Heaton & Kanamori (1999). MMI 6 = 0.092-0.18 PGA (g), MMI 7 = 0.18-0.34 PGA (g), MMI 8 = 0.34-0.65 PGA (g).

Table 7: Identification of the vulnerability rates of forest to the earthquake.

	MMI 6	MMI 7	MMI 8
Tree Mortality (Allen, 1999)	0.6%	11.7%	24%
Tree Mortality (Allen, 2020)	3%	4%	5%
Total average	1.8%	7.85%	14.5%

3.4.2 Wildfire vulnerability

Unlike the earthquake data, the wildfire data lacks intensity levels. Consequently, no distinctions are made between wildfire intensities when assessing the vulnerabilities of different land-use classes. To maintain consistency across hazards, the vulnerability rates for urban areas and cropland are assumed to be identical.

Based on destruction rates of buildings due to a wildfire by Kramer, Mockrin, Alexandre & Radeloff (2019), the damage rate of urban area is assumed to be 13.7%. Kramer et al. (2019) found minimal differences in destruction rates between densely populated urban areas and those surrounded by wildlands. Therefore, no distinction is made between dense urban areas (surrounded by urban area) and Wildland-Urban Interface (Urban area surrounded by wildland, e.g. forest). The same damage rate is applied to cropland. Based on Kiely et al. (2021), the damage rate of forest due to a wildfire is assumed to be 100%.

3.4.3 Summary of the calculation of the expected annual loss

To provide an overview of explanations of the calculation of the EAL discussed above, these will be summarized in equations in this paragraph. First, the expected annual loss due to an earthquake was calculated through the losses of each land-use class, using Equation 2.

$$EAL_{Earthquake} = \sum_{i=1}^n (0.0021 * Exposure_i * Vulnerability_{i,MMI}) \quad (2)$$

In this equation, n represents the different land-use classes. The annual frequency of 0.0021 corresponds to the probability of the earthquake occurring. The exposure depends on the land-use type, and the vulnerability is a function of both the land-use type and the earthquake intensity (MMI).

Next, the EAL due to a wildfire was calculated using Equation 3.

$$EAL_{Wildfire} = \sum_{i=1}^n (Frequency_{WF} * Exposure_i * Vulnerability_i) \quad (3)$$

Again, n represents the different land-use classes. The annual frequency is based on the spatial distribution in the hazard data. Both the exposure and vulnerability are dependent on the land-use type.

Finally, the total EAL for the independent hazards scenario is determined by summing the EAL from earthquakes and wildfires (Equation 4):

$$EAL_{Total} = \sum_{i=1}^n (0.0021 * Exposure_i * Vulnerability_{i,MMI}) + \sum_{i=1}^n (Frequency_{WF} * Exposure_n * Vulnerability_n) = EAL_{Earthquake} + EAL_{Wildfire} \quad (4)$$

This equation provides the total EAL by simply adding the damages caused by earthquakes and wildfires.

3.5 Cascading hazards scenario: hazard, vulnerability and expected annual loss

In the second scenario, the risk of cascading hazard interactions between earthquakes and landslides on the Island of Java is assessed. As in the first scenario, the spatial overlap of these hazards is determined, to identify areas affected solely by earthquakes and areas impacted by both earthquakes and landslides (Figure 8).

As this scenario concerns a cascading hazard relation rather than an independent hazard relation, the interaction between the hazards and also the impacts are a bit more complex. Specifically, the occurrence of landslides is partially dependent on the occurrence of earthquakes. Next to earthquakes being a trigger for landslides, precipitation can also induce landslides. In Figure 8, these two different landslide layers are combined into one landslide layer, as this map only represents the spatial overlap between the hazards and does not consider hazard or impact interactions. Because of the trigger relationship between earthquakes and landslides, the probabilities cannot simply be added up as in the independent hazard scenario. This will be elaborated on in the next paragraph.

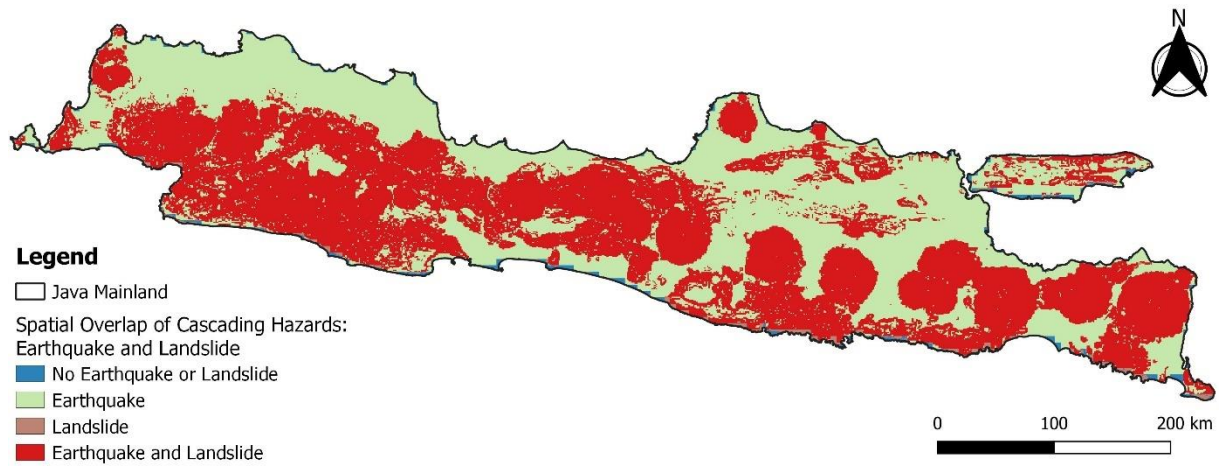


Figure 8: Spatial overlap of the earthquake and landslides on Java, in the cascading hazards scenario.

3.5.1 Hazard probabilities

To capture the relationship between consecutive hazards, specifically an earthquake followed by a landslide, an equation to calculate the conditional probability of a landslide is derived from Marzocchi, Garcia-Aristizabal, Gasparini, Mastellone & Di Ruocco (2012). In the equation, E_1 refers to the landslide and E_2 to the earthquake. The equation and corresponding explanation by Marzocchi et al. (2012) are as follows:

“We consider two different threatening events, whose occurrence is E_1 and E_2 . In general, the probability of E_1 occurrence (H_1) can be written as

$$H_1 = Pr(E_1) = Pr(E_1 | E_2) Pr(E_2) + Pr(E_1 | \bar{E}_2) Pr(\bar{E}_2) \quad (5)$$

where Pr represents a probability or a distribution of probability, and \bar{E}_2 means that the event E_2 does not occur.”

The equation by Marzocchi et al. (2012) can be divided into two parts. In the first part, $Pr(E_1 | E_2)$ represents the probability that a landslide (E_1) occurs given that the earthquake (E_2) occurs. $Pr(E_2)$ denotes the probability of the earthquake occurring. The product of these two terms is provided in the landslide dataset from UNEPGRID (2022) as the annual frequency of landslides triggered by earthquakes (with a return period of 500 years). In the second part, $Pr(E_1 | \bar{E}_2)$ represents the probability that a landslide occurs given that an earthquake does not occur, which is given in the landslide dataset from UNEPGRID (2022) as the annual frequency of landslides triggered by

precipitation. $Pr(\bar{E}_2)$ represents the probability that the earthquake does not occur, which is 474/475 (as opposed to the occurrence of the earthquake, which is 1/475).

The final annual hazard probability for locations on Java where only an earthquake occurs is 0.0021 (1/475). For locations where both an earthquake and a landslide can occur, the annual probability is (Equation 5):

$$Pr(\text{Earthquake}) + H_1 \quad (6)$$

Where $Pr(\text{Earthquake})$ is 0.0021 and H_1 is calculated using the equation above based on Marzocchi et al. (2012).

3.5.2 Vulnerabilities of landslides and dynamic vulnerability

As previously mentioned, the relationships between cascading hazards are more complex than those between independent hazards, as hazard and impact interactions must be considered in a risk assessment. Dynamic vulnerability can arise in scenarios where multiple hazards occur within a specific spatial and temporal frame. According to de Ruiter & van Loon (2022), there are three types of dynamic vulnerability, one of which involves the dynamics of vulnerability due to consecutive hazards. In this type, the first hazard affects the vulnerability at the time of the second hazard in the same location. This relationship is complex and depends on the location, its environment, and the types of assets present, making it challenging to account for in the risk assessment within the timeframe of this research. Moreover, although assets are more vulnerable during the second event as they have not recovered from the first event, their value also decreases due to the initial damage. Given the complexity and time required to accurately model this dynamic vulnerability, it is not included in this risk assessment. Therefore, vulnerability rates for both hazards will be used as if this were a single hazard risk assessment, similar to the approach in the independent hazards scenario.

For the EAL due to the earthquake, the same vulnerabilities as in the independent hazards scenario can be used. However, new vulnerability rates must be defined for EAL due to landslides. Several studies on the vulnerability of buildings to landslides, such as those by Glade (2003), Jakob, Stein, and Ulmi (2012), and Mavrouli and Corominas (2010), focus on the intensity and characteristics of the rock and the type of landslide, which is too detailed for this risk assessment due to the lack of required data. A relevant landslide risk analysis for West Java by Ngadisih, Yatabe, Bhandary, and Dahal (2014) will be used in this research to determine vulnerability rates for urban areas and cropland. Ngadisih et al. (2014) applied a damage rate of 0.5 for buildings and 0.7 for agricultural land. Consequently, the average rate of 0.6 is adopted for the vulnerability of urban areas and cropland.

For the vulnerability rate of forest, a tree mortality rate by Allen (1999) was used, who found that the tree mortality caused by landslides was 16.9%.

3.5.3 Summary of the calculation of the expected annual loss

The calculation of the EAL in the cascading hazards scenario is summarized in this paragraph. Due to the cascading relationship between the earthquake and landslides, the hazard and impact relations are more complex than in the scenario with two independent hazards. However, due to time and resource constraints, this complexity cannot be fully addressed in this research. As described in Paragraph 3.5.1, the triggering effect of the earthquake on landslides is already considered in the provided data. The vulnerability interactions, on the other hand, are not incorporated into this research, as discussed in Paragraph 3.5.2. Therefore, the calculations for losses due to an earthquake remain the same as in Equation 2.

To find the expected annual loss due to landslides, the following equations are used:

$$EAL_{Landslide} = \sum_{i=1}^n (Frequency_{LS} * Exposure_i * Vulnerability_i) \quad (7)$$

Here, exposure and vulnerability depend on the type of land use, and $Frequency_{LS}$ is calculated by:

$$Frequency_{LS} = Frequency_{LS,EQ} + Frequency_{LS,PR} * \frac{474}{475} \quad (8)$$

Where $Frequency_{LS,EQ}$ represents the frequency of landslides triggered by earthquakes, $Frequency_{LS,PR}$ represents the frequency of landslides triggered by precipitation, and the fraction $\frac{474}{475}$ is based on the probability that the earthquake does not occur.

Finally, similar to the independent hazards scenario, the expected annual losses from both hazards are summed, as shown in the equation below:

$$EAL_{Total} = \sum_{i=1}^n (0.0021 * Exposure_i * Vulnerability_{i,MMI}) + \sum_{i=1}^n (Frequency_{LS} * Exposure_i * Vulnerability_i) = EAL_{Earthquake} + EAL_{Landslide} \quad (9)$$

3.6 Data sources

To conduct the multi-hazard risk assessment, several data sources have been used. The calculations of the expected annual loss required data of the hazards, the exposure and the vulnerability. This section will discuss the data collection in Paragraph 3.6.1 and the data quality in Paragraph 3.6.2.

3.6.1 Data collection and pre-processing

The datasets used for the susceptibility map can be found in Appendix A, in which the table denotes the data source, description and other information about the layers. The spatial distribution of the datasets used for comparing the two hazard interaction scenarios is shown in maps in appendix B. The risk assessment was performed using QGIS, and all spatial analyses mentioned in this methodology were executed within this program. After downloading and implementing the seven datasets in QGIS, the first challenge was the varying pixel sizes and grid offsets among the layers. To address this, the raster layers were aligned to a single reference layer, ensuring uniform pixel sizes (1.23 hectares⁵) and grid offsets. This alignment step is essential for summing the raster layers.

I will elaborate on some of the spatial data presented in Appendix A, as some datasets are more complex than others. This complexity is particularly evident in the two landslide layers. The landslide data of UNEPGRID (2022) consists of two parts: one layer indicating the annual frequency of landslides triggered by precipitation and another layer showing the annual frequency of landslides triggered by earthquakes. NGI (2013) elaborates on the methodology for obtaining the global landslide risk datasets for the Global Assessment Report on Disaster Risk Reduction 2013. They used the following equations to identify landslide hazards:

$$H_{NGIr} = (S_r * S_l * S_h * S_v) * T_p \quad (10)$$

$$H_{NGIe} = (S_r * S_l * S_h * S_v) * T_s \quad (11)$$

These equations consider susceptibility factors S (e.g. lithology) and the precipitation factor (T_p) in the first equation and the seismic conditions (T_s) in the second equation. The seismic conditions are

⁵ In aligning the raster layer, the reference layer should be the one with the smallest pixel size, which was 1.23 hectares (110.73 metres * 110.73 metres) in this case. The unit of hectares was converted from the original unit, which was degrees (0.000992 degrees * 0.000992 degrees).

defined by the Peak Ground Acceleration (PGA), i.e. T_s increases when the PGA becomes larger. The NGI (2013) report used earthquake data of the expected PGA with a return period of 500 years. The data is categorized as follows: Low, Medium, High, Very High, which can be seen in Table 8 (NGI, 2013; Fraser, et al., 2017).

Table 8: Categorization of the annual frequency of the landslide hazard data.

Hazard category	Annual frequency per km ² (original data)	Frequency in GIS (this research)
Low	<0.00018	0.00009
Medium	0.00018 – 0.00032	0.00025
High	0.00032 – 0.00075	0.000535
Very high	>0.00075	0.001

Additionally, modifications were necessary for the land-use data provided by Copernicus (2019). In their original land-use data layer, there were some rectangles of built-up area in the east of Java (Appendix C). Besides the fact that these areas seem too square to be a real built-up area, they are located near and/or on a volcano which is actually covered by trees. Therefore, the rectangles of built-up area, indicated in Appendix C by the black circles, are changed to forest. This adjustment prevents overestimation of the expected annual loss, as the value of urban areas is significantly higher than that of forests.

3.6.2 Data quality

The data used in this multi-hazard risk assessment has a crucial influence on the final results. Several aspects of data quality are important to mention. Firstly, temporal accuracy is important to consider, especially for the land-use data sourced from Copernicus in 2019. This dataset, while comprehensive, may not fully capture recent changes in land use over the past five years. Although the primary hazard data layers (wildfires, landslides, and earthquake) are relatively recent and up to date, any updates in land-use patterns could potentially impact the assessment outcomes.

Another critical consideration was the alignment of raster layers' resolutions. Initially, these layers varied in resolution, which required aligning them to a uniform resolution to execute the raster calculations. This process, although necessary, may have introduced slight alterations to the original data, influencing the precision of the results to some extent. In contrast to the land-use dataset being slightly outdated, it does have a good resolution with pixels of 1.23 hectares, contributing to detailed results of the risk assessment.

Thirdly, a notable challenge involved the categorical distinctions within the land-use data, in regard to determining the exposure. The dataset did not differentiate between residential and industrial urban areas, but had all built-up areas in one single category. This simplification could affect the accuracy of vulnerability assessments, as residential and industrial areas probably vary in vulnerabilities and economic values.

In the case of the data of wildfire frequency, there could be a limitation. The dataset which was used covered only 20 years of historical data, which may not fully capture long-term trends of wildfires that could impact the risk assessment.

Despite these challenges, the assessment uses reliable data. All datasets came from trusted organizations known for their thorough data collection and analysis methods. This ensures confidence in the hazard data used, leading to reliable risk assessment results.

In conclusion, while the data used in this study provides a solid foundation for multi-hazard risk assessment, there are some limitations that researchers should consider. In Chapter 5, I elaborate on the limitations of this study.

4. Results of the multi-hazard risk assessment

In this chapter, the results of the multi-hazard risk assessment on Java are shown and discussed. First, I present the results of the hazard susceptibility analysis in Section 4.1. For both the independent hazard scenario and the cascading hazard scenario the expected annual losses are shown in maps, which will be discussed separately in Sections 4.2 and 4.3. Lastly, the results of both multi-hazard scenarios are compared in Section 4.4.

4.1 Hazard susceptibility analysis

As indicated in the introduction of Chapter 3, the first step of the multi-hazard risk assessment focused on identifying the types of hazards affecting Java. This section presents and discusses the outcomes of this identification process.

The map depicts how many combinations of the seven hazards, mentioned in 3.1, can arise in a certain area (Figure 9). It is crucial to note that the map does not include all potential natural hazards in Java, primarily due to data limitations. In addition, this map is heavily simplified in the sense that it is a summation of different hazard maps, just to show how many hazards can occur in a certain area and to give an indication of the distribution of the occurrence of multiple hazards. It does not account for the intensities or frequencies (probabilities) of these hazards, which are critical factors influencing multi-hazard risk assessments. The interactions between hazards, another crucial consideration, are also not represented in this map.

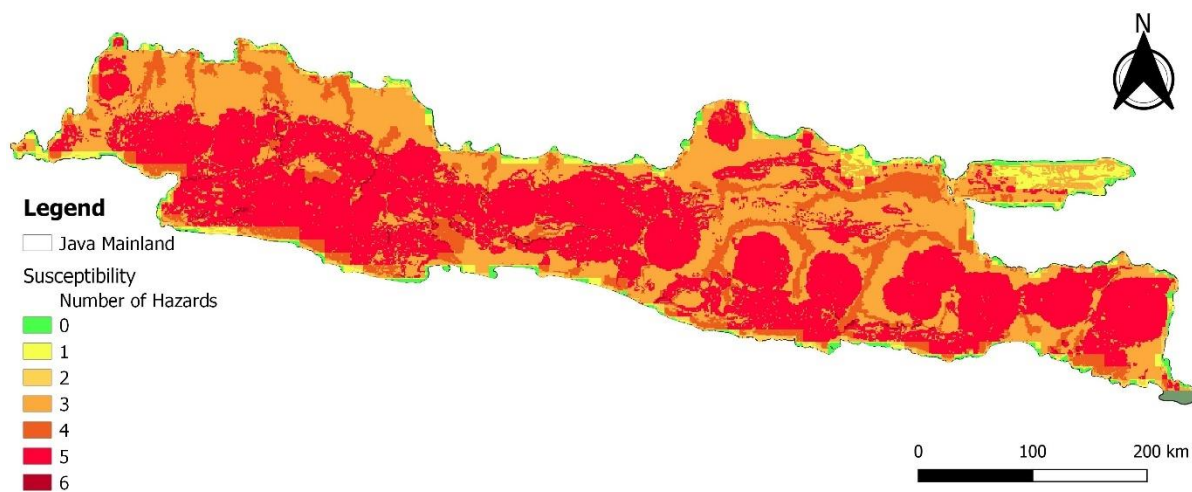


Figure 9: Susceptibility map of Java based on seven natural hazards. The map shows the spatial distribution multiple hazards possibly arising on Java⁶.

In Figure 9, the susceptibility map of Java is presented⁷. It can be seen that the biggest areas are characterized by the possible occurrence of five hazards as well as three hazards, which can also be found in Table 9. Based on this map, there are no obvious patterns in the distribution. However, it roughly shows that the south and middle part of Java deal with more hazards than the north and north-east part of Java. Table 9 shows the percentages of land coverage per number of hazards. In addition, the most frequent hazard combinations per number of hazards are shown. For three hazards, the most

⁶ In the far south-east of Java, a small part of the land does not indicate any number of hazards. This is a consequence of the raster alignment; some hazard datasets did not include this part of the island and it got lost in the raster alignment.

⁷ To preserve hazard data near the coast of Java, a buffer size of 1.5 kilometres has been set around the mainland of Java.

common combination is Earthquake, Wildfire and Volcanic hazard and for five hazards the most common combination is Landslide Eq., Landslide Pr., Earthquake, Wildfire and Volcanic hazard.

It is important to recognize that this map provides an initial, simplified overview of hazard distribution on Java and does not account for hazard intensities or frequencies. Variations in spatial distribution and the differential impacts of hazards on various assets are considerations that are addressed in the methodology (Sections 3.3-3.5) of this risk assessment, from which the results are discussed in the following sections in this chapter.

Table 9: Occurrence of the hazard combinations on Java.

Nr of hazards	Total land area (square kilometres)	% Total land area	Most frequent hazard combination (% area with the same number of hazards)
0	3021.5 ⁸	2.17%	None of seven hazards (100%)
1	4627.6	3.32%	Earthquake (89.1%), Coastal flood (8.2%)
2	3081.0	2.21%	Wildfire and Volcanic hazard (60.2%), Landslide Pr. and Earthquake (17%)
3	47934.5	34.39%	Earthquake, Wildfire and Volcanic hazard (95.6%)
4	14240.9	10.22%	River flood, Earthquake, Wildfire and Volcanic hazard (67.8%), Landslide Pr., Earthquake, Wildfire and Volcanic hazard (25.5%)
5	65523.8	47.01%	Landslide Eq., Landslide Pr., Earthquake, Wildfire and Volcanic hazard (99.9%)
6	949.3	0.68%	River flood, Landslide Eq., Landslide Pr., Earthquake, Wildfire and Volcanic hazard (100%)
Total	139378.7	100%	

4.2 Scenario of independent hazards

To obtain the results for the independent hazards scenario, the methods outlined in Chapter 3 were implemented. The results are visualized in several maps, to provide a clear depiction of the spatial distribution of damages. In addition, to show the division between the damages caused by an earthquake and a wildfire there are two separate damage maps made for these two hazards.

In Figure 10, the expected annual loss due to an earthquake on Java is illustrated. The loss of urban area, cropland and forest ranges from 0 to 1500 US dollars per hectare. There are some large concentrated areas where the losses are expected to be the highest. If we compare these areas to the land-use map in Figure 6, it can be seen that the high loss areas correspond to the urban areas. It also corresponds to the fact that the urban areas have the highest economic values and are also the most prone to earthquakes in comparison to cropland and forest.

⁸ Due to the implemented buffer of 1.5 kilometres on Java this area is relatively large, as it includes some surface of the sea where no hazard (data) occurs.

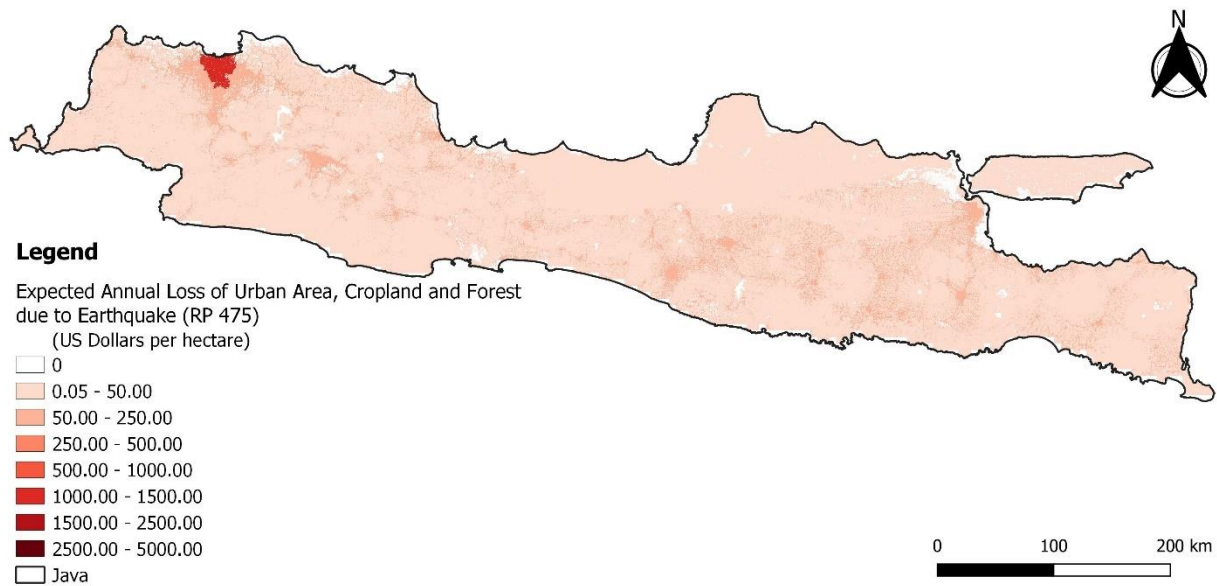


Figure 10: Spatial distribution of the Expected Annual Loss on Java due to earthquakes. The earthquake data uses a return period of 475 years.

Secondly, a map was generated to depict the expected annual loss from wildfires on Java (Figure 11). Here, losses across urban areas, croplands, and forests range from 0 to 5000 US dollars per hectare. In comparison the earthquake damages, the range of the losses is much higher. However, the damages done by a wildfire show a less clear spatial pattern than the damages done by an earthquake. It is noticeable that there are more areas where there is an expected annual loss of zero (white areas), reflecting the absence of wildfires in these regions over the past two decades. Many of these areas are partially urbanized, making them less susceptible to wildfire incursion.

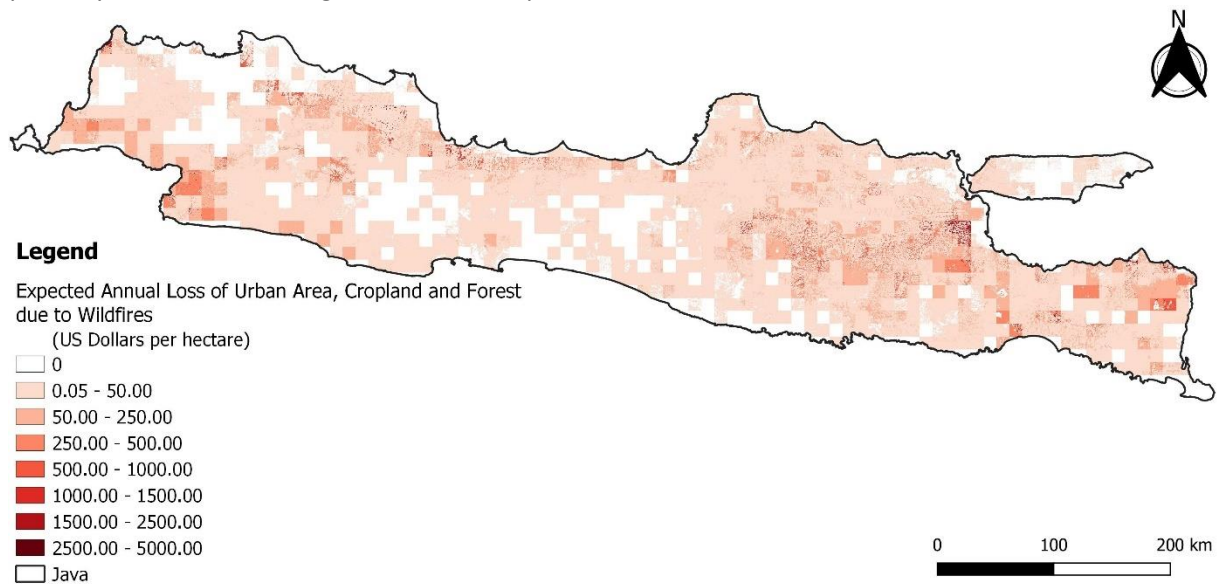


Figure 11: Spatial distribution of the Expected Annual Loss on Java due to wildfires.

Finally, the two maps were combined to obtain a final map of the expected annual loss on Java in the independent hazards scenario (Figure 12). In this scenario, the total expected annual loss of urban area, cropland and forest ranges from 0 to 5000 dollars per hectare. The map does not show one clear spatial pattern of the expected annual losses. It can be seen that there are again concentrated higher values of damage around the built-up areas. Additionally, significant areas of high damage are observed in the southwest and eastern parts of Java, predominantly encompassing forested regions.

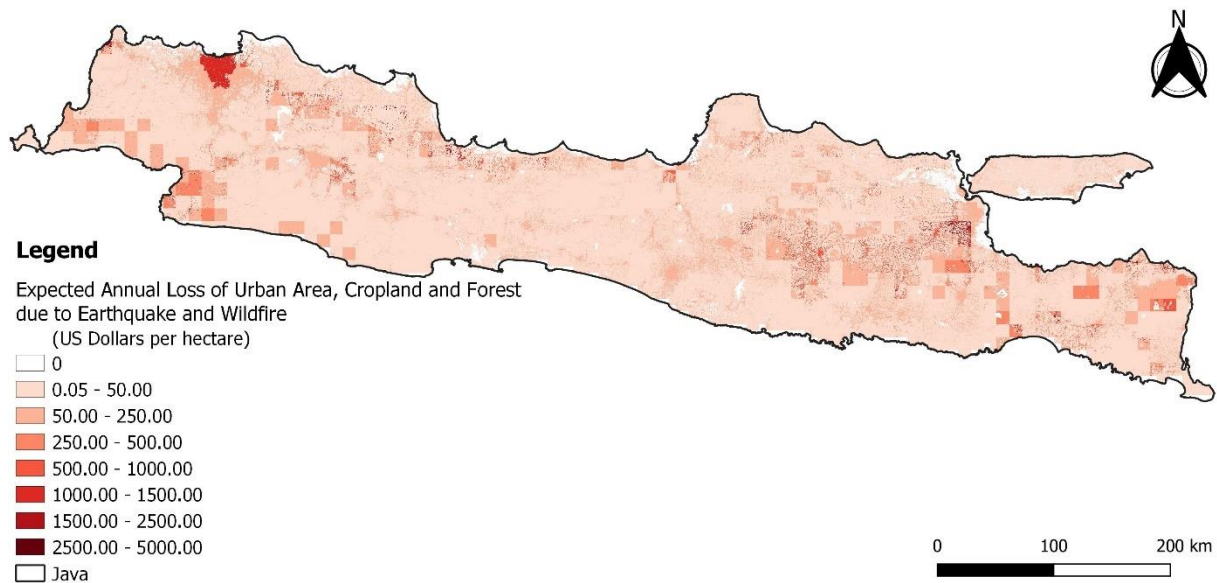


Figure 12: Spatial distribution of the total Expected Annual Loss on Java in the independent hazards scenario.

4.3 Scenario of cascading hazards

For the results of the cascading hazards scenario, the methods used can also be found in Chapter 3. Like in the first scenario, the results for this scenario are also shown in different maps, to visualize the spatial distribution of the expected losses. As the method to obtain the damages caused by an earthquake is the same for both scenarios, and the dynamic vulnerabilities are not taken into account in the cascading hazard scenario, the earthquake-induced loss map is identical to that of the first scenario (Figure 10). Consequently, in this section a map of damages caused by landslides and the final map of the damages caused by an earthquake and landslides combined can be found.

Figure 13 illustrates the outcomes of the landslide risk assessment across Java. The first thing to notice, is that in comparison to the earthquake and wildfire maps, a lot more areas have a value of zero loss in the landslide map. This disparity arises because landslides tend to occur more locally, influenced by diverse landscape and soil characteristics. In the most affected areas, damages are relatively low, namely between 0 and 50 US Dollars per hectare. However, there are some smaller areas which are more damaged with an expected annual loss up to 500 US dollars per hectare.

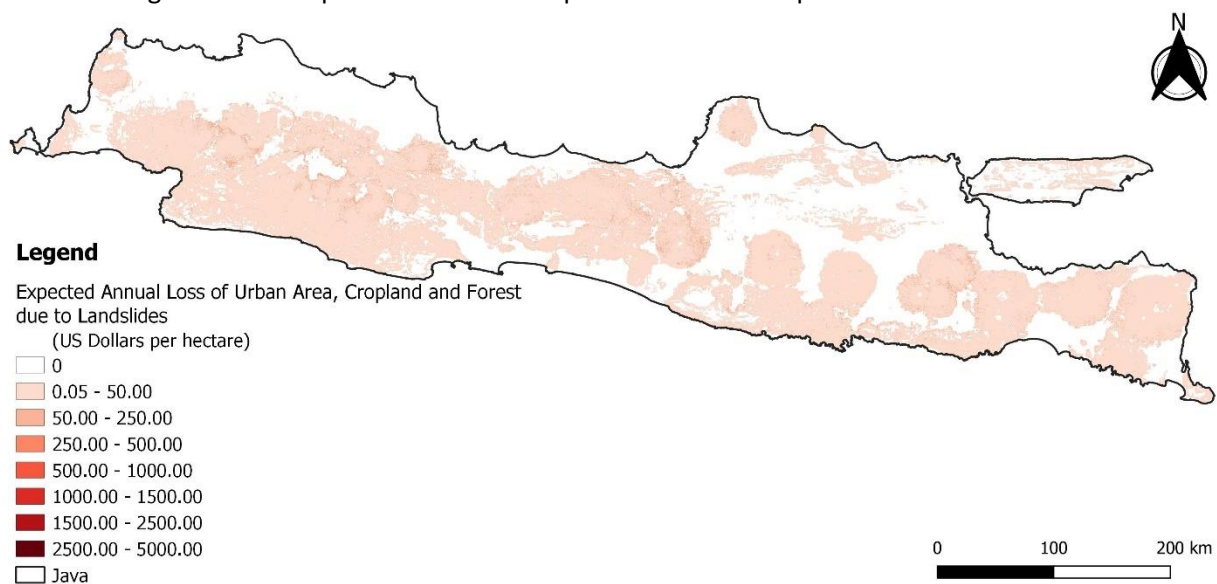


Figure 13: Spatial distribution of the Expected Annual Loss on Java due to landslides.

Combining the earthquake damage map (Figure 10) with the landslide damage map (Figure 13), Figure 14 presents the results for the cascading hazards scenario. In this scenario, the total expected annual loss of urban area, cropland and forest ranges from 0 to 1500 dollars per hectare. The overall pattern of this combined loss map resembles that of the earthquake-only scenario (Figure 10). This is due to the fact that there are some large areas which are affected by landslides but the damages are low, and there are only small local areas where the damage is much higher. Because of the pixel size it is hard to recognize the combination of earthquake and landslide damages in Figure 14.

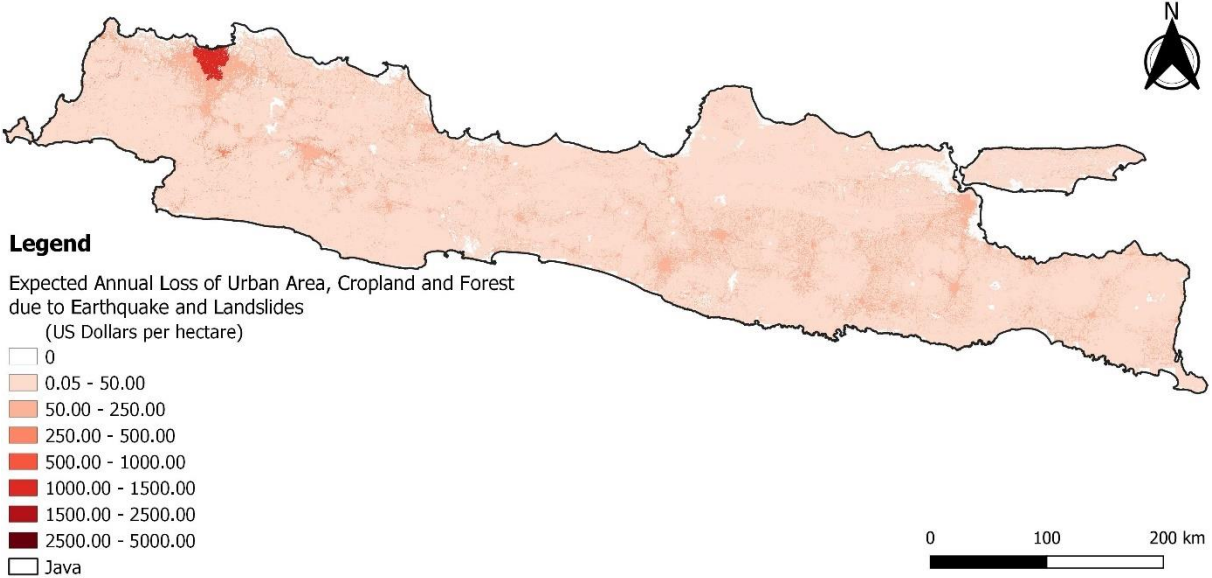


Figure 14: Spatial distribution of the total Expected Annual Loss on Java in the cascading hazards scenario.

4.4 Comparison between independency scenario and cascading scenario

Between the two examined scenarios, differences in hazard types and their interactions result in distinct spatial distributions, impacts, and expected annual losses. The most notable difference is the rang of damages, which is higher for the independent hazards scenario (up to 5000 US Dollars per hectare) than for the cascading hazards scenario (up to 1500 US Dollars per hectare).

Comparing the total expected annual losses between the two scenarios reveals both spatial similarities and differences (Figure 12 & Figure 14). For instance, in and around the city of Jakarta the damages are the same in both scenarios. However, the independent hazards scenario shows more concentrated areas of higher damages, particularly in the eastern and western part of the island. These concentrated areas contribute to the differences in damage ranges between the scenarios, with some regions experiencing higher damages but at a low density. Overall, the damages due to multi-hazard risk on Java seem to be bigger in the independent hazards scenario than in the cascading hazard scenario.

5. Conclusion and discussion

In this final chapter, the conclusion of this research is given, by answering the main research question and its sub-questions (Section 5.1). This is followed by the discussion in Section 5.2, which elaborates on assumptions made in the methodology, data quality and limitations, possible explanations of this research' results, comparisons with other literature, contributions of this study and recommendations for future research.

5.1 Conclusion

The goal of this research was to gain knowledge about current methods regarding multi-hazard risk and to explore the applicability of these methods in multi-hazard risk assessment. The central research question guiding this study was:

What are important aspects to improve in multi-hazard risk assessment methodologies?

This research question was supported by three sub-questions, which were the following:

1. *Which methods are used in previously performed research?*
2. *What are the current challenges in multi-hazard risk assessment?*
3. *What can we learn from the appliance of these methods to a new case study area, by comparing two scenarios of different hazard interactions?*

The first two sub-questions were examined in the literature review (Chapter 2). For the first sub-question, the review examined existing research on hazard interactions, multi-hazard risk assessment, and multi-hazard frameworks. It was found that numerous multi-hazard risk assessments have been conducted using various methodologies. The foundation of most multi-hazard risk assessments involves determining the hazards, exposure (assets) of the location, and the vulnerability of these assets to the hazards, similar to single-risk assessments. A common issue identified in many multi-hazard risk assessments is the separate estimation of risk for each hazard, followed by aggregation to determine the total multi-hazard risk. This approach often overlooks the interactions between hazards and the associated impacts (Hochrainer-Stigler, et al., 2023). In spite of the fact that some of the multi-hazard risk assessments disregard the hazard and impact interactions, there are several frameworks constructed by researchers which do take the complex interrelationships into account. Generally, these frameworks include steps such as identifying hazards and their interactions, identifying assets at risk, and analysing vulnerability. Frameworks also differ slightly amongst studies, some address identifying the spatial and temporal overlap as an important step and others address defining options for risk management as an important step. The first step in most of the frameworks, identifying the hazard interactions, heavily relies on determining the (trigger) relationships between hazards. From the literature review it appears that a wide range of terminology exists, addressing the same kind of interrelationships. However, hazard interactions are extensively studied, for example by Gill & Malamud (2014), who provide characterization of the interactions relationships between natural hazards.

The review of existing methods highlights several challenges in multi-hazard risk assessment. To sum up, there is no universal terminology addressing the hazard interactions, many risk assessments do not take hazard and impact interactions into account, and the applicability of existing frameworks is complex and not fully standardized.

To answer the last sub-question, frameworks typically provide the foundational steps for multi-hazard risk assessment. However, applying these frameworks to specific study areas is challenging, making the feasibility of performing accurate risk assessments lower than desired. The methods can be applied by following the most general steps outlined in Chapter 3, but must be supported by additional

background literature. Especially when comparing two scenarios of hazard interaction, it appears that significant additional sub-steps were needed for the implementation of hazard interaction calculations. These hazard interactions were much simpler for the independent hazard interaction than for the cascading hazard interaction. In this research, only two different hazard interactions were examined, both including two hazards. It is likely that alternative calculations are needed when examining other hazard interactions, and it becomes even more complex if more than two hazards are included.

In conclusion, in the current development phase of multi-hazard risk assessment the possibilities are to follow a structured approach: identifying hazards and their interactions, calculating the probabilities of the multi-hazard scenarios, determining exposure of the study area, assessing vulnerability (excluding dynamic vulnerability), and finally calculating the expected damages to occur in the multi-hazard scenario. Although current frameworks offer general guidelines, it can be concluded that there are important aspects to improve multi-hazard risk assessment methodologies. The main aspects to improve in multi-hazard risk assessments are having access to methods for hazard interaction calculations and dynamic vulnerability calculations. Many additional sub-steps are needed to apply the frameworks to specific case study areas and specific hazard interactions. Future research could focus on developing general yet location-specific frameworks to improve the accuracy and applicability of multi-hazard risk assessments. Additionally, frameworks could be tailored to different types of hazard interactions, creating specific frameworks for each interaction type that incorporate the base calculations for the probability of specific multi-hazard scenarios.

5.2 Discussion

First, I will reflect on the methodologies used for the assessment in terms of assumptions, limitations and data quality. To perform a feasible multi-hazard risk assessment and obtain the results of the case study, several assumptions were made in this research:

1. It was assumed that the economic values of forest and cropland do not significantly differ across various regions of Java, unlike urban areas where value varies throughout the regions.
2. Due to the lack of specific data, the vulnerability of cropland was assumed to be equivalent to that of urban areas, based on the presence of infrastructure and machinery. This assumption was extended to wildfires and landslides for consistency.
3. Vulnerability rates for urban areas were obtained from data pertaining to building types in the Philippines, assuming similarity with Indonesian structures.

These assumptions were necessary to make for the implementation of the risk assessment, due to lack of data and literature, and time available for this research. This could have led to less accuracy in the results. Next to the assumptions made to conduct the methodology, different data resources were used for the risk assessment. Data quality of the spatial data was already addressed in Section 3.3, but not yet for the exposure and vulnerability data used. The NPV and GDP were used for the monetary values of forest, cropland and urban area. The accuracy of the values of the NPV, for forest and cropland, is debatable as it is quite difficult to determine a value for these land-use types as it depends on many aspects. Additionally, there are many differences in types of forest and cropland and thus probably in their monetary values, but they are all taken as one category in this research. This could have led to less accuracy in the calculations. The values of the NPV are obtained from an article published in 2021, which is fairly recent but the values could be more accurate coming from 2023 or 2024. As mentioned before, GDP is a quite standard measure to find the economic exposure (Ward, et al., 2020). The GDP data is up to date as it is from 2023 so the use of GDP should positively affect the accuracy of the damage calculations. However, not all types of exposure were used in this case study (e.g. infrastructure, people), which could have led to an underestimation of the damages.

In addition to exposure, the vulnerability of the assets was a crucial component in the damage calculations. To find the vulnerability rates of each land-use type to each natural hazard, various

resources have been used. It is debatable whether these vulnerability rates are accurate enough. Few studies were done on the vulnerability of land-use types to natural hazards, which led to some assumptions made mentioned above. Additionally, not all vulnerability rates were conducted for the island of Java or similar areas, but also obtained from other locations like the United States. It can be questioned whether vulnerability rates determined based on analysis in totally different areas can be applied to other locations like Java. Therefore, vulnerability rates of land uses should be investigated further to find rates which are applicable to a certain area with a certain hazard.

Next to the debatable accuracy of the vulnerability rates, dynamic vulnerability was not included in the damage calculations due to its complexity, despite its recognized importance. De Ruiter & van Loon (2022) stated that dynamic vulnerability approaches are currently rare in risk assessments, but including this in future research is important since incorporating dynamic vulnerability will increase the accuracy of risk assessments and therefore improve risk management. To elaborate shortly on possible calculations of dynamic vulnerability, Marzocchi et al. (2012) say that Equation 5, used for the landslide probability (H1), is generated for the interaction between hazards, but argue that “similar ideas may be straightforwardly extrapolated also for vulnerability assessment”. However, it would be too complex to find an accurate vulnerability relation and therefore I did not apply this in my risk assessment. But it is still an important aspect to investigate further in future research, which may be built on the equation by Marzocchi et al. (2012).

Second, I will discuss the results of the multi-hazard risk assessment. The susceptibility map in Section 4.1 illustrates the potential occurrence of seven hazards across Java, yet no single area is subject to all seven. This relates to the geographic and environmental specificity required for each hazard type, preventing that there is one area where all hazards can occur simultaneously. There is probably no combination of geographic and environmental factors in which all seven hazards can arise.

In Section 4.4, the analysis revealed that damages are higher in the independent hazards scenario compared to the cascading hazards scenario. This finding contrasts with the intuitive expectation that cascading hazards, which typically affect the same areas, would result in more substantial damage. This overlap in affecting the same areas is not necessarily the case in an independent hazards scenario, but the spatial overlap between the earthquake and wildfires was quite large. The difference lies in the types of damages considered: while both scenarios include earthquake damages, the independent scenario incorporates wildfire damages, whereas the cascading scenario considers landslide damages. The wildfire damages in the independent scenario were significantly higher than the landslide damages in the cascading scenario. Additionally, the landslide damages were fairly localized in its spatial distribution, leaving big areas with a damage of zero due to landslides, and thereby contributing to the overall lower damage estimates in the cascading scenario. The cause of the damages by landslides being lower than by wildfires could have multiple origins, which could be methodological as well as geographical. The vulnerability rates used in this assessment for landslides and wildfires could be different in reality, the damage caused by landslides could be underestimated and the damage caused by wildfires could be overestimated. Additionally, the spatial distribution of landslides, occurring mostly on higher elevated areas, could be a clarification of the low damages. Generally, higher elevated areas are less populated and thus less assets are at risk (Cohen & Small, 1998). Moreover, the hazard of wildfires is more spread out throughout the island than the hazard of landslides, and thus reaches more assets (Appendix B, Figure 16 & 17). However, the wildfire damages can be overestimated as the large resolution of the wildfire data leads to inclusion of large urban areas in the damages, while these may not be affected that greatly. These methodological choices and geographical characteristics have a big influence on the results. Other natural hazards, in the same two scenarios, would have led to different results of the expected annual loss between the scenarios.

Third, I will examine related literature and look for similarities and differences to my findings. One of the main conclusion drawn from this research was the fact that multi-hazard risk assessment often ignored the interactions between hazards and their impacts. An important step for incorporating

hazard interactions in the risk assessment, is aligning the spatial resolutions of all hazard data (Shi, et al., 2015). By normalizing the unit of damage (US Dollars per hectare) and using unified spatial resolutions, multi-hazard damages can be accumulated per location. Shi et al. (2015) created global maps of expected annual multi-hazard risk, showing their results by grid cells as well as by geographic units (administrative borders). When you compare these maps, you can see clear differences in the spatial distribution of the expected risks and therefore the loss of detail when using administrative borders rather than grid cells. This underscores the importance of the Modifiable Areal Unit Problem, mentioned in Section 2.2 (Openshaw, 1984). Parts of the framework of Liu et al. (2016) were implemented, but their use of administrative borders in their case study was not adopted. To improve accuracy in the multi-hazard risk assessment, the damages were calculated per grid cell in this research.

In relation to study area specific research, limited multi-hazard risk assessments have been conducted on Java. Examples include Nugraha et al. (2017) and Tauhid et al. (2017), both of which employed overlay and weighting methods without considering the probability of the multi-hazard scenarios or dynamic vulnerability. Most existing studies, such as those by Ningsih et al. (2023) and Marfai et al. (2008), focus solely on susceptibility mapping rather than providing comprehensive damage assessments, which is only one of the first steps in a multi-hazard risk assessment. This underscores the early stages of multi-hazard risk assessment development for Java, highlighting the contribution of this research in advancing the field.

Another important thing to notice is the significance of economic damage to low income households versus high income households. In this research, I did not account for social welfare and therefore utility in the damage calculations. The value of money for a low income household is bigger than for a high income household, and thus damages by natural hazards have a greater impact on the lives of low income households than those of high income households (Kind, Wouter Botzen, & Aerts, 2017). This underestimation of damage to low income households should be considered in future research.

Finally, this study significantly contributes to the literature by providing insights into the risks posed by multiple hazards in Java. Understanding these multi-hazard risks is crucial for effective risk management and mitigation strategies, not only for Java but for other regions as well. The findings emphasize the need for refined assessment methodologies to achieve more accurate and actionable results. Therefore, there are several recommendations which can be done for future research on this topic. First, establishing a universal glossary for hazard interactions by governmental or authoritative bodies is essential to prevent misuse of terminology. Second, developing frameworks that distinguish between different types of hazard interactions could improve the applicability of assessments. Third, integrating dynamic vulnerability into risk assessments is critical for more accurate damage predictions. Fourth and final, in this research only two multi-hazard scenarios were examined, but there are many other hazards interactions possible. These different scenarios require different methods to calculate the probability of the scenario, which should be investigated in future research by performing multi-hazard risk assessments.

References

- Ahamed, M. S., Sarmah, T., Dabral, A., Chatterjee, R., & Shaw, R. (2023, March 7). Unpacking systemic, cascading, and compound risks: A case based analysis of Asia Pacific. *Progress in Disaster Science*, 18, 100285.
- Aksha, S. K., Resler, L. M., Juran, L., & Carstensen Jr, L. W. (2020, January 20). A geospatial analysis of multi-hazard risk in Dharan, Nepal. *Geomatics, Natural Hazards and Risk*, 11(1), 88-111.
- Allen, R. B., Bellingham, P. J., & Wiser, S. K. (1999, March 1). Immediate damage by an earthquake to a temperate montane forest. *Ecology*, 80(2), 708-714.
- Allen, R. B., MacKenzie, D. I., Bellingham, P. J., Wiser, S. K., Arnst, E. A., Coomes, D. A., & Hurst, J. M. (2020). Tree survival and growth responses in the aftermath of a strong earthquake. *Journal of Ecology*, 108(1), 107-121.
- Baky, M. A., Islam, M., & Paul, S. (2020). Flood hazard, vulnerability and risk assessment for different land use classes using a flow model. *Earth Systems and Environment*, 4, 225-244.
- Berkeley Economic Review. (2019, March 17). *Disaster Risk Reduction and Management in Indonesia*. Retrieved from Berkeley Economic Review: UC Berkeley's Premier Undergraduate Economics Journal: <https://econreview.berkeley.edu/disaster-risk-reduction-and-management-in-indonesia/>
- Botzen, W. W., Deschenes, O., & Sanders, M. (2019, June 25). The economic impacts of natural disasters: A review of models and empirical studies. *Review of Environmental Economics and Policy*.
- BPS-Statistics Indonesia. (2023, November). *Indonesia's economic growth in Q3-2023 4.94 percent (y-on-y)*. Retrieved from BPS-Statistics Indonesia: <https://www.bps.go.id/en/pressrelease/2023/11/06/2000/indonesia-s-economic-growth-in-q3-2023-4-94-percent--y-on-y-.html>
- BPS-Statistics Indonesia. (2024, February 15). *[2010 Version] Quarterly GDRP At Constant Market Price by Industrial Origin in Province (Billion Rupiah), 2010-2023*. Retrieved from BPS-Statistics Indonesia: <https://www.bps.go.id/en/statistics-table/1/MjIwNiMx/-2010-version--quarterly-gdrp-at-constant-market-price-by-industrial-origin-in-province--billion-rupiah---2010-2023.html>
- Center For Hazards and Risk Research at Columbia University. (2005). *Indonesia Natural Disaster Profile*. Retrieved from Center For Hazards and Risk Research at Columbia University: <https://www.ldeo.columbia.edu/chrr/research/profiles/indonesia.html>
- Ciurean, R., Gill, J., Reeves, H. J., O'Grady, S., & Aldridge, T. (2018). Review of multi-hazards research and risk assessments.
- Cohen, J. E., & Small, C. (1998, November 24). Hypsographic demography: the distribution of human population by altitude. *Proceedings of the National Academy of Sciences*, 95(24), 14009-14014.
- Copernicus. (2019). *Data viewer*. Retrieved from Copernicus: Land Monitoring Service: <https://land.copernicus.eu/en/map-viewer?product=333e4100b79045daa0ff16466ac83b7f>

- Cutter, S. L. (2018, October 26). Compound, cascading, or complex disasters: what's in a name? *Environment: Science and Policy for Sustainable Development*, 60.6: 16-25.
- De Angeli, S., Malamud, B. D., Rossi, L., Taylor, F. E., Trasforini, E., & Rudari, R. (2022, April 15). A multi-hazard framework for spatial-temporal impact analysis. *International Journal of Disaster Risk Reduction*, 73, 102829.
- De Groot, R., Brander, L., Van Der Ploeg, S., Costanza, R., Bernard, F., Braat, L., . . . Van Beukering, P. (2012, July). Global estimates of the value of ecosystems and their services in monetary units. *Ecosystem services*, 1(1), 50-61.
- de Ruiter, M., & van Loon, A. (2022, July 4). The challenges of dynamic vulnerability and how to assess it. *IScience*, 25(8).
- Dilley, M., Chen, R. S., Deichmann, U., Lerner-Lam, A., Arnold, M., Agwe, J., . . . Yetman, G. (2005). Natural disaster hotspots: a global risk analysis. *The World Bank*.
- European Environment Agency. (2017). *Climate Change, Impacts and Vulnerability in Europe: an Indicator-based Report*.
- FEMA. (2024). *Expected Annual Loss*. Retrieved from FEMA: National Risk Index: <https://hazards.fema.gov/nri/expected-annual-loss>
- Fraser, S., Douglas, J., Simpson, A., Kuijper, M., Winsemius, H., Burzel, A., . . . Giraud, P. (2017). *ThinkHazard! Methodology Report*. World Bank Group & GFDRR.
- Fujimi, T., & Aulady, M. F. (2019, January 1). Earthquake loss estimation of residential buildings in Bantul regency, Indonesia. *Jàmbá: Journal of Disaster Risk Studies*, 11(1), 1-10.
- Gallina, V., Torresan, S., Critto, A., Sperotto, A., Glade, T., & Marcomini, A. (2016, March 1). A review of multi-risk methodologies for natural hazards: Consequences and challenges for a climate change impact assessment. *Journal of environmental management*, 168, 123-132.
- GAR. (2017). *GAR 2017 Atlas Risk Data and Software Download Facility*. Retrieved from Global Assessment Report on Disaster Risk Reduction: <https://risk.preventionweb.net/>
- GFDRR. (2015, June 24). *VO-GLOBAL-GFDRR*. Retrieved from GFDRR: https://www.geonode-gfdrmlab.org/layers/hazard:volc_globalproximalhazard_wgs84#more
- GFDRR. (2016, July 27). *SS-GLOBAL-MUIS-500*. Retrieved from GFDRR: https://www.geonode-gfdrmlab.org/layers/hazard:ss_muis_rp0500m#license-more-above
- Gill, J. C., & Malamud, B. D. (2014, August 14). Reviewing and visualizing the interactions of natural hazards. *Reviews of Geophysics*, pp. 52(4), 680-722.
- Gissing, A., Timms, M., Browning, S., Crompton, R., & McAneney, J. (2022). Compound natural disasters in Australia: A historical analysis. *Environmental Hazards*, 21(2), 159-173.
- Glade, T. (2003). Vulnerability assessment in landslide risk analysis. *Erde*, 134(2), 123-146.
- Global Earthquake Model (GEM). (2023). *Global Seismic Hazard Map 2023.1 vs 2019.1*. Retrieved from OpenQuake Map Viewer: <https://maps.openquake.org/map/gshm-2023-1/#7/-7.544/108.442>

- Hochrainer-Stigler, S., Trogrlić, R. Š., Reiter, K., Ward, P. J., de Ruiter, M. C., Duncan, M. J., . . . Gottardo, S. (2023, April 26). Toward a framework for systemic multi-hazard and multi-risk assessment and management. *Iscience*, 26(5).
- Jakob, M., Stein, D., & Ulmi, M. (2012). Vulnerability of buildings to debris flow impact. *Natural hazards*, 60, 241-261.
- Kiely, L., Spracklen, D. V., Arnold, S. R., Papargyropoulou, E., Conibear, L., Wiedinmyer, C., . . . Adrianto, H. A. (2021, December 2). Assessing costs of Indonesian fires and the benefits of restoring peatland. *Nature Communications*, 12(1), 7044.
- Kind, J., Wouter Botzen, W. J., & Aerts, J. C. (2017, April). Accounting for risk aversion, income distribution and social welfare in cost-benefit analysis for flood risk management. *Wiley Interdisciplinary Reviews: Climate Change*, 8(2), e446.
- Kramer, H. A., Mockrin, M. H., Alexandre, P. M., & Radeloff, V. C. (2019, July 30). High wildfire damage in interface communities in California. *International journal of wildland fire*, 28(9), 641-650.
- Leroy, S. A. (2006, December). From natural hazard to environmental catastrophe: Past and present. *Quaternary International*, 158(1), 4-12.
- Liu, B., Siu, Y. L., & Mitchell, G. (2016, March 3). Hazard interaction analysis for multi-hazard risk assessment: a systematic classification based on hazard-forming environment. *Natural Hazards and Earth System Sciences*, 16(2), 629-642.
- Marfai, M. A., King, L., Singh, L. P., Mardiatno, D., Sartohadi, J., Hadmoko, D. S., & Dewi, A. (2008, January 4). Natural hazards in central Java province, Indonesia: an overview. *Environmental Geology*, 56, 335-351.
- Marzocchi, W., Garcia-Aristizabal, A., Gasparini, P., Mastellone, M. L., & Di Ruocco, A. (2012, January 26). Basic principles of multi-risk assessment: a case study in Italy. *Natural Hazards*, 62, 551-573.
- Mavrouli, O., & Corominas, J. (2010, October 6). Rockfall vulnerability assessment for reinforced concrete buildings. *Natural Hazards and Earth System Sciences*, 10(10), 2055-2066.
- Naguit, M., Cummins, P., Edwards, M., Ghasemi, H., Bautista, B., Ryu, H., & Haynes, M. (2017, August 1). From source to building fragility: post-event assessment of the 2013 M7. 1 Bohol, Philippines, Earthquake. *Earthquake Spectra*, 33(3), 999-1027.
- Negulescu, C., Smai, F., Quique, R., Hohmann, A., C. U., Guidez, R., . . . Grandjean, G. (2023). VIGIRISKS platform, a web-tool for single and multi-hazard risk assessment. *Natural Hazards*, 115(1), 593-618.
- Ngadisih, Yatabe, R., Bhandary, N. P., & Dahal, R. K. (2014). Integration of statistical and heuristic approaches for landslide risk analysis: a case of volcanic mountains in West Java Province, Indonesia. *Georisk: Assessment and Management of Risk for Engineered Systems and Geohazards*, 8(1), 29-47.
- NGI. (2013). *Landslide Hazard and Risk Assessment in El Salvador - UNISDR Global Assessment Report 2013 - GAR13*. Geneva, Switzerland: UNISDR.

- Ningsih, R. L., Wulan, P. Y., Haq, A. H., Ihsan, F. N., Kusuma, R. W., Farhan, R., . . . Haryono, E. (2023). Multi-Hazard Susceptibility Analysis of Bantul Regency. *Jurnal Geografi Gea*, 23(1), 8-18.
- Nugraha, A. L., Hani'ah, H. A., & Pratiwi, R. D. (2017, July 25). Assessment of multi hazards in Semarang city. *AIP Conference Proceedings*, Vol. 1857, No. 1.
- Nugroho, A., Triana, L., Fitrah, A. U., & Hamid, A. H. (2022, July). Multi-hazard perception during COVID-19: Evidence from rural communities in West Sumatra, Indonesia. *International Journal of Disaster Risk Reduction.*, 77, 103075.
- OCHA. (2020, April 8). *Indonesia - Subnational Administrative Boundaries*. Retrieved from HUMANITARIAN DATA EXCHANGE (HDX): <https://data.humdata.org/dataset/cod-ab-idn>
- Openshaw, S. (1984). The modifiable areal unit problem. *Concepts and techniques in modern geography series.*, No. 38.
- OpenStreetMap tiles. (2024). *Index of tile logs*. Retrieved from Planet OSM: https://planet.openstreetmap.org/tile_logs/
- Pescaroli, G., & Alexander, D. (2018). Understanding compound, interconnected, interacting, and cascading risks: a holistic framework. *Risk analysis*, 38(11), 2245-2257.
- Randell, H., Jiang, C., Liang, X. Z., Murtugudde, R., & Sapkota, A. (2021, September). Food insecurity and compound environmental shocks in Nepal: Implications for a changing climate. *World development*, 145, 105511.
- RASOR Project. (2013). *Northern Italy case study*. Retrieved from Rapid Analysis And Spatialization Of Risk: <http://www.rasor-project.eu/rasor-case-studies-northern-italy/>
- Röthlisberger, V., Zischg, A. P., & Keiler, M. (2017, November 15). Identifying spatial clusters of flood exposure to support decision making in risk management. *Science of the total environment*, 598, 593-603.
- Sadegh, M., Moftakhari, H., Gupta, H. V., Ragno, E., Mazdiyasn, O., Sanders, B., . . . AghaKouchak, A. (2018, May 18). Multihazard scenarios for analysis of compound extreme events. *Geophysical Research Letters*, 45(11), 5470-5480.
- Shi, P., Yang, X., Liu, F., Li, M., Pan, H., Yang, W., . . . Meng, Y. (2015, January 1). Mapping multi-hazard risk of the world. *World atlas of natural disaster risk*, 287-306.
- Statista. (2022, June). *Share of population in Indonesia in 2020, by main island*. Retrieved from Statista: <https://www.statista.com/statistics/1318607/indonesia-population-share-by-main-island/>
- Tauhid, C. D., Fathani, T. F., & Legono, D. (2017, September). Multi-disaster risk analysis of Klaten regency, Central Java, Indonesia. *Journal of the Civil Engineering Forum*, Vol. 3, No. 3.
- Tilloy, A., Malamud, B., Winter, H., & Joly-Laugel, A. (2019, September). A review of quantification methodologies for multi-hazard interrelationships. *Earth-Science Reviews*, 196, 102881.
- UNEPGRID. (2022, July 11). *WESR-RISK*. Retrieved from UN environment programme: GRID Geneva: https://wesr.unepgrid.ch/?project=MX-XVK-HPH-OGN-HVE-GGN&theme=color_light&language=en

- UNEPGRID. (2024, February 26). *WESR-RISK*. Retrieved from UN environment programme: GRID Geneva: https://wesr.unepgrid.ch/?project=MX-XVK-HPH-OGN-HVE-GGN&theme=color_light&language=en
- UNISDR. (2009). *UNISDR terminology on disaster risk reduction*. Geneva, Switzerland: United Nations International Strategy for Disaster Reduction.
- Volcano Hazards Program. (1905). *USGS*. Retrieved from The Modified Mercalli Intensity (MMI) Scale assigns intensities as ...: <https://www.usgs.gov/media/images/modified-mercalli-intensity-mmi-scale-assigns-intensities>
- Wald, D. J., Quitoriano, V., Heaton, T. H., & Kanamori, H. (1999). Relationships between peak ground acceleration, peak ground velocity, and modified Mercalli intensity in California. *Earthquake spectra*, 15(3), 557-564.
- Wang, J., He, Z., & Weng, W. (2020, September 3). A review of the research into the relations between hazards in multi-hazard risk analysis. *Natural Hazards*, 104, 2003-2026.
- Ward, P. J., Blauhut, V., Bloemendaal, N., Daniell, J. E., de Ruiter, M. C., Duncan, M. J., . . . Winsemius, H. C. (2020, April 22). Natural hazard risk assessments at the global scale. *Natural Hazards and Earth System Sciences*, 20(4), 1069-1096.
- World bank. (2021). *Indonesia*. Retrieved from Climate Change Knowledge Portal: <https://climateknowledgeportal.worldbank.org/country/indonesia/vulnerability>
- World Environment Situation Room. (2023, March 28). *WESR: Risk*. Retrieved from UN environment programme: <https://wesr.unepgrid.ch/?project=MX-XVK-HPH-OGN-HVE-GGN&language=en>
- Zhang, Y., Hao, Z., & Zhang, Y. (2023, March 1). Agricultural risk assessment of compound dry and hot events in China. *Agricultural Water Management*, 277, 108128.
- Zuzak, C. E., Goodenough, Stanton, C., Mowrer, M., A.Sheehan, Roberts, B., . . . Rozelle., J. (2023). *National Risk Index Technical Documentation*. Washington, D.C.: Federal Emergency Management Agency.

Appendix

A. Summarizing table of spatial data sources used for this research

Data and format	Description	Data source
Administrative boundaries (vector layer)	Data of administrative boundaries of Indonesia, including provinces and districts.	(OCHA, 2020)
Land use (raster layer, resolution of 110.73 x 110.73 metres)	Land-use data of Java from 2019.	(Copernicus, 2019)
Landslides triggered by earthquakes (raster layer, resolution of 928.36 x 928.36 metres)	This dataset includes an estimate of the annual frequency of landslide triggered by earthquakes.	(UNEPGRID, 2022)
Landslides triggered by precipitation (raster layer, resolution of 928.36 x 928.36 metres)	This dataset includes an estimate of the annual frequency of landslide triggered by precipitations.	(UNEPGRID, 2022)
Earthquake hazard (raster layer, resolution of 5570.08 x 5570.08 metres)	The Global Earthquake Model (GEM) Global Seismic Hazard Map (version 2023.1) depicts the geographic distribution of the Peak Ground Acceleration (PGA) with a 10% probability of being exceeded in 50 years.	(Global Earthquake Model (GEM), 2023)
Wildfire hazard (raster layer, resolution of 11139.89 x 11139.89 metres)	The density of fires is reported as the count of fires per km ² between 2003 and 2022.	(UNEPGRID, 2024)
Coastal flood (raster layer, resolution of 928.16 x 928.16 metres)	Coastal flood data with a return period of 500 years.	(GFDRR, 2016)
River flood (raster layer, resolution of 1002.86 x 1002.86 metres)	Riverine flood data with a return period of 500 years.	(GAR, 2017)
Volcanic hazard (raster layer, resolution of 11139.88 x 11139.88 metres)	Volcanic hazard data for e.g. pyroclastic flows, lahars, lava. Date of last eruption and maximum VEI are used to generate the Volcanic Hazard Level, which is assigned to the area within 100km radius of the volcano. This dataset does not include data for hazard from volcanic ash.	(GFDRR, 2015)

B. Maps of the original hazard datasets used in the two multi-hazard scenarios

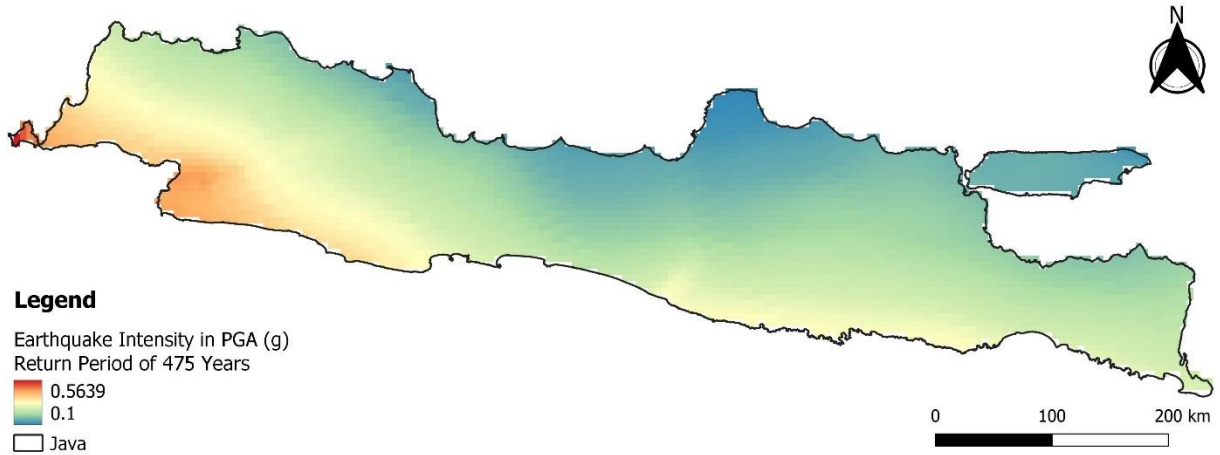


Figure 15: Earthquake hazard data used for the risk assessment. The data uses a return period of 475 years for the earthquake, and the intensity of the earthquake is expressed in Peak Ground Acceleration (PGA), using gravity (g) as an (acceleration) unit. Retrieved from Global Earthquake Model (GEM) (2023).

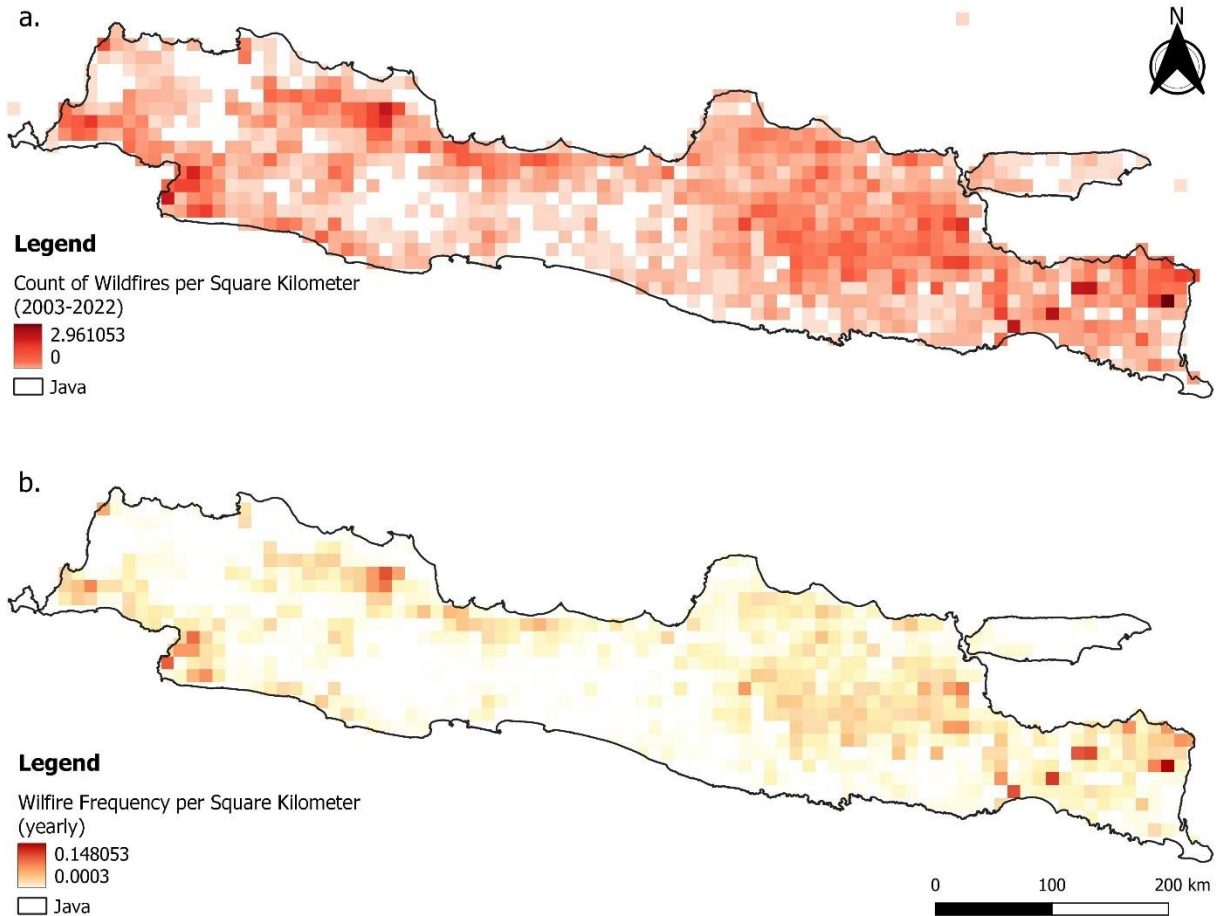


Figure 16: Wildfire hazard data used for the risk assessment. In Figure 16a, the original data is shown. The data gives the count of fires per square kilometre, over the years of 2003 till 2022. In Figure 16b, the modified data is shown. The data was modified to the annual frequency of wildfires per square kilometre, by dividing the original hazard data by 20 (years). Retrieved from UNEPGRID (2022).

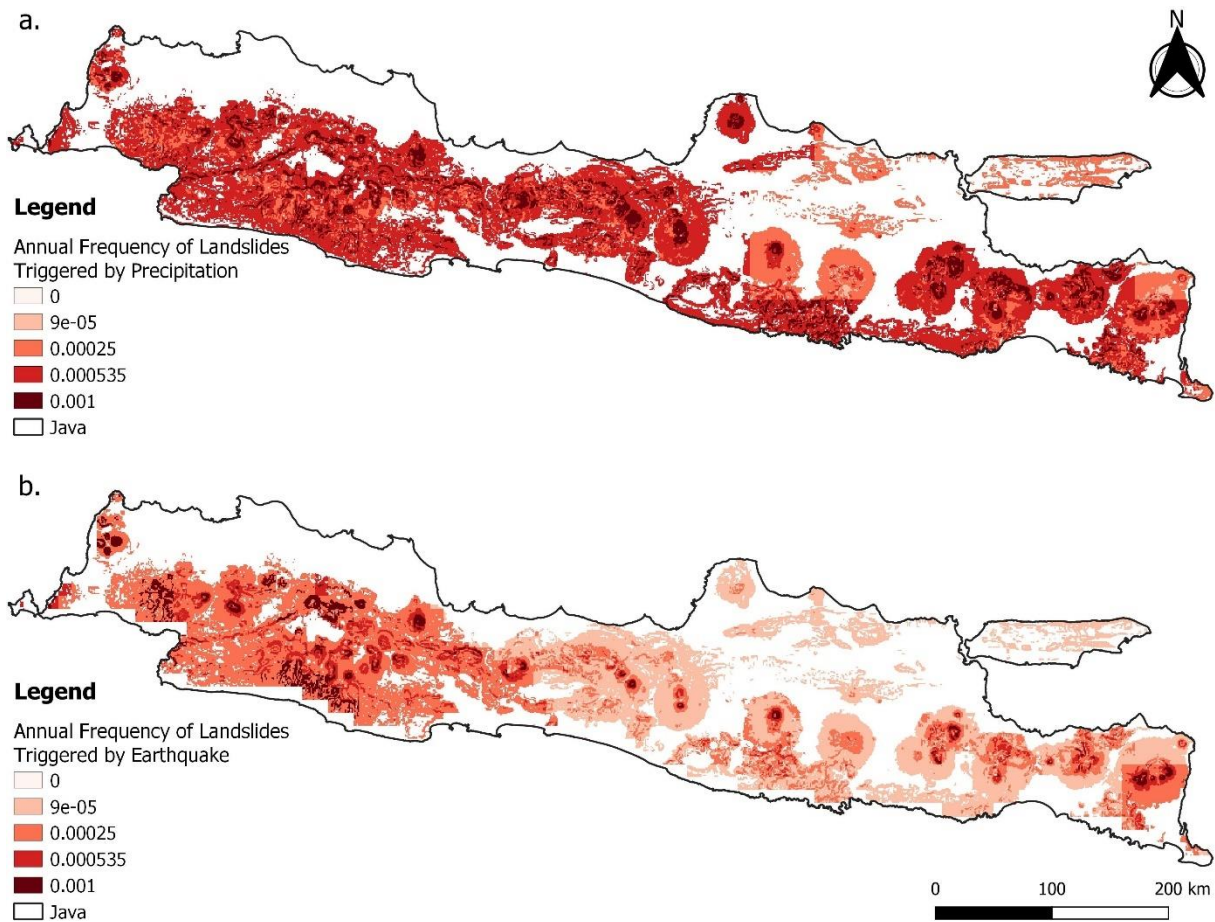


Figure 17: Landslide hazard data used for the risk assessment. In Figure 17a, the expected annual frequency of landslides which are triggered by precipitations is shown. In Figure 17b, the expected annual frequency of landslides which are triggered by earthquakes is shown. For both maps, the original categories (1-7) are modified to actual frequencies, following (Fraser, et al., 2017), which is described in Section 3.6. Retrieved from UNEPGRID (2022).

C. Original land-use dataset

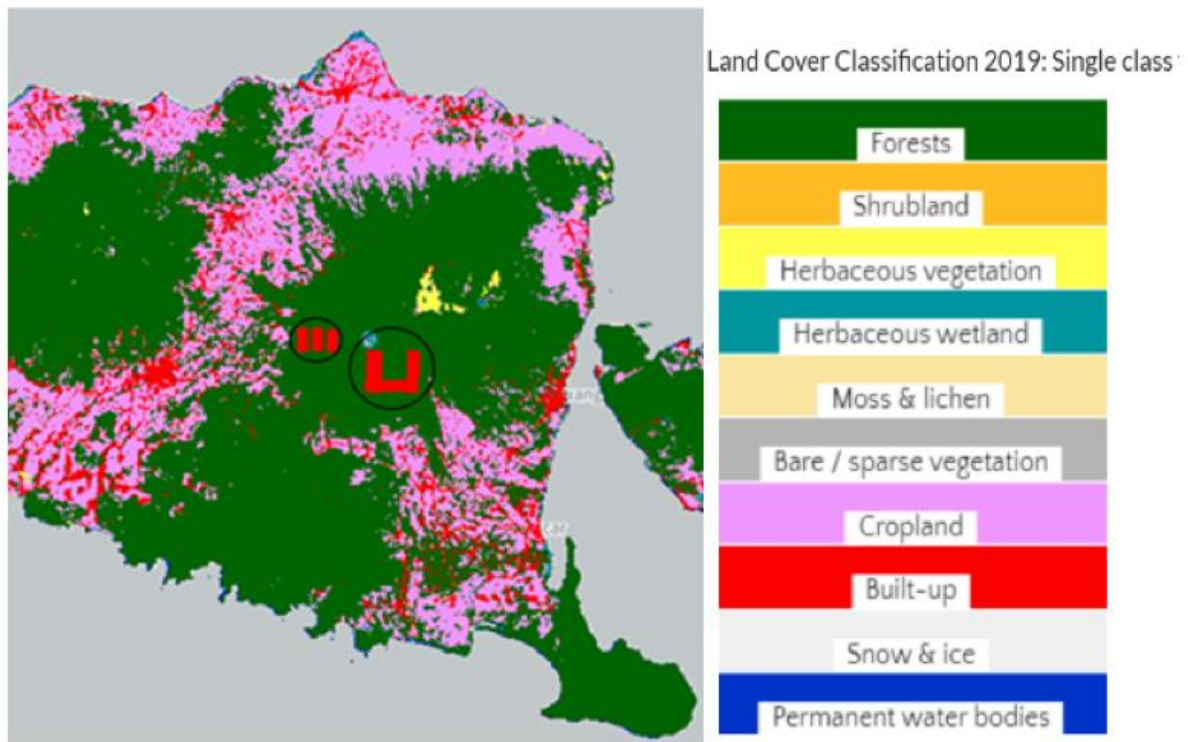


Figure 18: Original land-use dataset from Copernicus (2019), with the two black circles indicating the errors of urban area. Besides the fact that these areas seem too square to be a real built-up area, they are located near and/or on a volcano which is actually covered by trees. Therefore, the rectangles of built-up area, indicated by the black circles, are changed to forest.